IONIC RELATIONSHIPS OF ENTEROMORPHA INTESTINNALIS L.

David R. Black

A Thesis Submitted for the Degree of PhD
at the
University of St Andrews

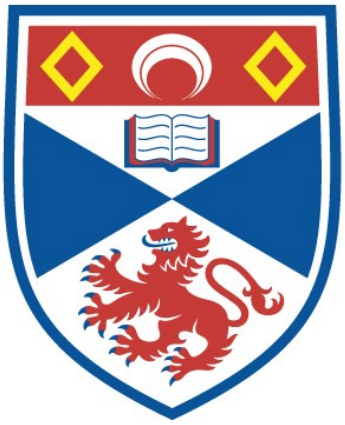

1971

IONIC RELATIONSHIPS OF

ENTEROMORPHA INTESTINALIS L. (LINK)

BY

DAVID R. BLACK.

A thesis submitted to the University of St. Andrews
for the degree of Doctor of Philosophy.

Gatty Marine Laboratory and
The Department of Botany,
University of St. Andrews. September 1971.

ProQuest LLC.
789 East Eisenhower Parkway
P.O. Box 1346
Ann Arbor, MI 48106 – 1346

DECLARATION

I hereby declare that the following thesis is based upon work done by me, that the Thesis is my own composition, and that it has not been previously presented for a Higher Degree.

The research was carried out at the Gatty Marine Laboratory, University of St. Andrews, under the supervision of Dr. D.C. Weeks.

. . . . . .

CAREER.

I graduated from the University of Salford in July 1968 with an Upper Second Class Joint Honours Degree in Chemistry and Botany. I was awarded a Natural Environment Research Council Studentship for 3 years research at the University of St. Andrews.

In October 1968 I was admitted as a Research Student under Ordinance General No. 12 and under Resolution of the University Court 1967 No. 1.

CERTIFICATE

I certify that David Robert Black has spent twelve terms of research under my direction, that he has fulfilled the conditions of Ordinance General No. 12 and Resolution of the University Court 1967, No. 1, and that he is qualified to submit the accompanying Thesis in application for the Degree of Doctor of Philosophy.

. . . . . .

ACKNOWLEDGEMENTS.

The author wishes to record his gratitude to Dr. D.C. Weeks of the Department of Botany, University of St. Andrews, for supervising the work presented in this Thesis and for his enthusiasm and availability for discussion throughout the whole project.

He also wishes to thank Professors J.A. MacDonald of the Department of Botany and M.S. Laverack of the Department of Marine Biology, for providing the facilities for research; the technical staff at the Gatty Marine Laboratory, especially Mr. J. Brown, for their cheerful help and assistance; and last but not least, my wife for all her help.

FOR NOW WE SEE THROUGH A GLASS, DARKLY;

1 Cor. 13v 12.

CONTENTS

ABSTRACT

The green alga Enteromorpha intestinalis (L. Link) has been observed to grow over a wide range of salinities, from 0.1% to 100% sea water, the optimum growth range being between about 30% and 70% sea water. The range of salinities in which the alga occurs is unusually wide for a marine alga, and an investigation of its ionic relationships was therefore undertaken. Measurements have therefore been made of concentrations of the major ions (Na, K and Cl) in the plant cells and in sea water together with measurements of cell membrane potential and ion flux rates.

Measurements of the electrical potential difference across the plasmalemma and the influx and efflux of each ion indicate that K and Cl are actively imported and Na actively exported over the whole salinity range. Estimates of cell permeability to the passive diffusive fluxes of these three ions alone have been used

to explain the origin of the cell membrane potentials over the range of salinities. Tracer ion kinetics are taken as showing that the tonoplast is more permeable than the plasmalemma to each ion.

The ion fluxes against their electrochemical potential gradients consist of at least two components, one active, the other passive, the passive component has been calculated, for each ion, from the Goldman flux equations. The remaining putative active flux components have been compared with the measured active fluxes and the interlinkages of the latter have been determined. None of the active transport mechanisms for each ion appear to be electrogenic neither do they appear to be 1:1 coupled exchange transport as all the active fluxes are affected by the lowering of temperature and by certain metabolic inhibitors. Use of such inhibitors has enabled division of the fluxes into their component parts. A component of the active

K influx and a component of the active Na efflux are linked through a ouabain sensitive transport mechanism. A further component of the active K influx is ouabain insensitive but is dependent upon Cl, and further, a part of this Cl dependent K influx requires light while the remainder does not. The active Cl influx has a light dependent component, part of which appears to require both K and Na specifically, the remainder being cation independent.

This interlinkage of active fluxes appears to be maintained at all dilutions of sea water as the influxes and effluxes of each ion remain in constant proportion to one another and to the fluxes of other ions over the whole salinity range investigated. The ratio of internal concentration to external concentration, for each ion, increases with increasing dilution although the ratios of the internal ions to one another remain reasonably constant. When plants are maintained in solutions of varying sodium to potassium ratio the internal sodium to potassium

ratio differs markedly from that found in plants growing in sea water; the plants in such experimental solutions, however, appear to be able to tolerate these internal ionic ratios and have remained healthy in such solutions for at least seven days. The majority of plants require a constant internal ionic environment for efficient functioning of their metabolism. This does not appear to be the case with E. intestinalis which may account for its ability to inhabit regions of widely varying salinity.

1. INTRODUCTION.

The green alga Enteromorpha intestinalis (L. Link) is widely distributed in the temperate zone and is a common littoral alga around the British coast and in tidal estuaries. The life cycle consists of an alternation of morphologically identical generations. Each consists of a small holdfast and a relatively large tubular thallus with walls one cell thick. The thallus consists largely of mature cells uniform in shape and size; each cell of the alga is exposed directly to the bathing medium and must, therefore, osmoregulate individually. The alga occurs over a range of salinities which is unusually wide for a marine alga, it has been found in fresh water ponds, in estuaries, in the sea and in salinities more concentrated than sea water. There is no evidence yet that genetically distinguishable types of alga occupy different parts of the salinity range. The relatively simple morphology of the alga makes it suitable for physiological studies of its

ionic relationships which are interesting because of the salinity range over which the alga is found.

The aim of the work was to ascertain the nature of ionic control and the interlinkage of ion fluxes and how this varied over a wide salinity range.

The study of ion transport in plant cells has been reviewed by Dainty (1962), Briggs, Hope and Robertson (1961) and for marine algae more recently by Gutknecht and Dainty (1968). These and most other authors approach the subject from the point of view of the electrochemistry of the plant cell in its medium. This is not the only way in which ionic relationships in plant cells may be studied; an alternative approach is that of irreversible thermodynamics, e.g. Katachalsky and Curran (1965) and Hope (1971). This approach, however, has at least two major drawbacks limiting its usefulness. All the various forces acting on a species of ion are described in terms of frictional coefficients.

Since these coefficients are purely phenomenological it is often difficult to relate them to measurable kinetic properties of matter in the cell system. The second limitation is that detailed knowledge about nearly all the thermodynamic variables on both sides of the membrane and an ability to vary most of them is required. Both are difficult to achieve in practice, especially in cells as small as those in E. intestinalis where varying the internal ionic concentrations for example, is extremely difficult. Control of the thermodynamic variables has been achieved, however, in squid axon and the giant unicell Valonia by Baker, Hodgkin and Shaw (1962) and Gutknecht (1966) respectively.

The electrochemical, or classical thermodynamic, approach involves the use of parameters which are not phenomenological but are in fact measurable quantities such as concentration, electrical potential difference and rates of movement of ions (flux rates). The classical thermodynamic approach is, however, more limited

in scope. It is essentially a theory describing systems in equilibrium or undergoing reversible processes and is particularly applicable to closed systems. I have assumed, as have many other workers, that the system under consideration is not too far from equilibrium for a simple electrochemical approach to be invalid.

The electrochemical approach considers that an ion species will always be acted upon by at least two physical forces; the chemical potential gradient and the electrical potential gradient. In fact at least two other physical forces should be considered,that of a viscous drag exerted by flowing water in which the ions are dissolved and the effects of movement of other ion species. These last two physical forces are taken to be small or constant and are neglected in this simple treatment. (The ion interaction is quite large, but fairly constant, in the high salinities of sea water and cell protoplasm of E. intestinalis). Further to reduce the effect of water flow attempts have

been made to work at, as near as possible, water flux equilibrium.

The movements of an ion species in response to its electrochemical potential gradient is known as passive ion movement. An ion will, of course, move down its electrochemical potential gradient, that is, from a region of high electrochemical potential to a low one. Thus if in a membrane-bound cell there is a lower electrochemical potential for a given species of ion inside the cell than out there will be a net flux of those ions into the cell. If there is no difference in the electrochemical potential across the cell membrane there will be no net flow of these ions from one side of the membrane to the other, that is passive influx is equal (and opposite) to passive efflux and that ion species is then in passive flux equilibrium. The electrochemical potential difference E, between the inside and the outside of the membrane can be predicted from the Ussing-Teorell equation 1.1 (Ussing, 1949 and Teorell, 1949).

$$E = \frac{RT}{zF} \log_e \frac{J_{io}\, a_o}{J_{oi}\, a_i} \quad - - - \quad 1.1$$

where R = gas constant

T = temperature degrees K

z = algebraic valency of the ion

F = the Faraday

J_{io} = influx (flux from inside to outside)

J_{oi} = efflux (flux from outside to inside)

a_o = activity of the ion outside the cell

a_i = activity of the ion inside the cell

In fact concentrations and not activities are used throughout this work as the latter are extremely difficult to measure inside plant cells.

In a living system, such as a plant cell, other ion species will also be involved. The passive diffusion of all ion species will generate a potential across the membrane, this is discussed below.

In nearly all living cells there is a fifth force which acts upon the ions and affects their movements. This force is generally termed

active transport. I have adopted a simple definition of active transport; when work has been done on an ion, by the cell, the ion may be considered to have been actively transported. A criterion for active transport is discussed below. Such active transport is obligately linked to metabolism, but of course passive transport can also be directly and is always indirectly dependent upon metabolism. Ions which are moved by active transport are no longer moving under the influence of their electrochemical potential gradient alone. That is such actively transported ions are no longer moving purely passively. Such an ion flux against its electrochemical potential gradient will therefore consist of an active and a passive component.

If the mechanism for active transport is situated at a cell membrane then ions that are actively transported will no longer obey the Ussing-Teorell equation. Thus the calculated electrochemical potential difference for that ion

will not be the same as the measured electrochemical potential difference. The difference E between the calculated e.m.f. and the measured e.m.f. indicates the minimal energy gradient against which the ion must be moved by active transport into or out of the cell. The sign of the difference indicates the direction of transport. There is therefore a criterion for determining whether active transport is occuring and if it is, its direction. If there is no significant statistical difference between the observed and measured e.m.f. then the ion can be said to be assorting passively. A difference in the observed and measured e.m.f.s can, however, be due to active transport or to a 1:1 coupled exchange transport of the ion, or to one or more of the assumptions made above being incorrect. These two forms of transport can be distinguished as inhibition of a putative active flux (but not the passive flux) by metabolic inhibitors is inconsistent with a 1:1 coupled ion exchange transport.

The passive diffusion of ions will generate a potential across the cell membrane. If this is the only source of potential and the assumptions of this approach are valid then the observed values of the membrane potential will be predictable from the Goldman equation 1.2, for all the major ions involved. In this case these are Na, K and Cl.

$$E_G = \frac{RT}{F} \ln \frac{P_K(K_o) + P_{Na}(Na_o) + P_{Cl}(Cl_i)}{P_K(K_i) + P_{Na}(Na_i) + P_{Cl}(Cl_o)} \quad --- \quad 1.2$$

Where the symbols have the same meaning as in equation 1.1 and

E_G = e.m.f. calculated from the Goldman equation

P = The permeability of the ion given by the suffix

(J_o)=The external concentration of the ion J

(J_i)=The internal concentration of the ion J

In many cells a substantial part of the observed membrane potential is generated by active transport of one or more ions by a membrane component bearing a greater net charge on one half of its cyclic "journey" across the cell membrane.

Such an ion transport system is said to be electrogenic. In practise it is difficult to establish, beyond doubt, the existence of an electrogenic ion transport system. If the measured membrane potential falls when active transport is inhibited, for instance by a metabolic inhibitor, then it is probable that the transport system contributes to the measured cell membrane potential i.e. it is electrogenic. If the measured membrane potential does not fall then the transport system is probably not electrogenic.

Studies employing the criteria described above have been used to investigate the interlinkage of the various active flux components and their relationships with metabolism have also been determined. Radioactive tracers have been employed to determine influx and efflux rates separately for each ion. The methods of calculation of these flux rates is discussed in the text, Section 2.8.

2. MATERIALS AND METHODS.

2.1. Collection of Plant Material.

Plants of *E. intestinalis* were collected from the South end of the East Sands, St. Andrews, Scotland, and were brought back to the laboratory in plastic bags. On return to the laboratory the plants were placed in filtered sea water at room temperature and left to stand until the sediment had settled. Visibly damaged and infected plants were rejected along with those which had sand grains in the tubular thalli. In order that the plants collected from the field at low tide on different days, and thus under different climatic conditions, could be compared directly, the plants were left to stand in filtered sea water at room temperature before being placed in the experimental solution. This pre-experimental equilibration enabled any subsequent physiological reaction to be considered as a reaction due to the experimental bathing solution.

The algae were removed from the sea water, after at least 24 hours equilibration, and blotted so as to remove as much surface water as possible before being placed in experimental bathing solutions. All plants were treated in this way before being placed in experimental solutions.

For both influx and efflux experiments mature vegetative portions of whole thalli, without their reproductive areas, were cut into lengths of about 1.5cm. These tubular pieces were then cut open lengthwise into a sheet one cell thick, which weighed about 0.005g., and were kept in illuminated sea water before use.

Dainty, Hope and Denby (1960), among others, have shown that cell walls of Chara contain Na, K and Cl ions which may be distributed in the Donnan free space or in the water free space of the cell wall. From an analysis of pieces of whole thalli it is impossible to determine the distribution of ions in the wall

and in the cytoplasm and vacuole of the cells separately. The cells of E. intestinalis are too small to be able to extract the cytoplasm from the cells as did MacRobbie (1962) from Nitella. However, when E. intestinalis produces spores all the cytoplasmic contents are extruded from the cell leaving empty cell ealls. Spores are released from areas at the tip of the mature thallus and because spore release in field material is more or less synchronous (Christy and Evans, 1962) this enables large amounts of cell wall material free of protoplasm to be collected.

Such protoplasm free areas of thallus are easily recognised as they appear white in contrast to the dark green of the remaining vegetative thallus. Study of such material allows estimates of ion concentrations and ion flux rates in the cell walls alone to be made and compared with data for living material. This allows estimation of concentrations and flux rates of ions in the whole protoplasts to

be made.

2.2. Chemical Analyses.

The concentrations of the major constituent cell ions, K, Na and Cl, in the cells and bathing solutions were determined. Mature vegetative portions of whole thalli were used in the analyses as well as cell wall material alone. Gross analyses for ions could have been conducted by ashing the plants and measuring ion concentrations in the remaining ash. This method was not employed because K salts are volatile and might have been lost during the ashing process. The method chosen is described below.

Plants for analysis were removed from the experimental equilibrating solutions and were slit open along their lengths. The tissue was then cut into lengths of approximately 1cm. and blotted between two sheets of tissue paper by rolling a standard 52g. weight over the tissue. This procedure was adopted to prevent

excess surface solution being carried over into the digestion solution. The use of a standard weight to ensure uniform blotting of tissue was developed after a series of experiments described in Appendix 2 had been conducted. About 10g. of tissue treated in this way was weighed accurately and placed into a Quickfit 250ml. round bottomed flask containing 100ml. of 0.5M HNO_3 (Analar). The whole was then refluxed for two hours at the end of which time the flasks were allowed to cool to room temperature. A blank solution containing 0.5M HNO_3, but no tissue, was also treated in this way. The cool mixture was then filtered through a Watman No. 1 filter paper which had previously been washed with 0.5M HNO_3 and allowed to dry. This washing removed any ions which might have exchanged with Na, K or Cl or bound them to the surface of the paper. It is possible the ion binding sites on the filter paper material may have remained and may have retained some of the ions present in the un-filtered solution. If any ions were retained

in this way it was not detected by the analytical methods used. The filtrate was collected in flat bottomed glass tubes which were stoppered to await analysis. Cell wall material was treated in the same way as whole plant material.

K and Na were analysed using a Model A EEL Flame Photometer and calibrating solutions containing all three ions in concentrations similar to those being analysed. Cl was analysed in 10ml. aliquots of HNO_3 digest made to approximately 0.75M with respect to HNO_3. A potentiometric titration was carried out to determine Cl using an AgCl/AgCl sat./KNO_3 sat. reference electrode as a salt bridge and an Ag wire as a potential detector. An automatic digital titrator was used to deliver $AgNO_3$ titrant through a valve controlled by the potential between the two electrodes.

The total ionic concentration for each ion was calculated for the whole protoplast volume, taking the volume to be 0.61 ± 0.06 $cm^3/g.$ tissue as measured by light microscope and ^{14}C

mannitol technique, (see Appendix 3).

The method of analysis employing nitric acid releases bound ions as well as those which are osmotically free and "active". It is possible that bound ions, which do not contribute to the electrochemical potential gradient, could comprise a large proportion of the total and thus lead to misinterpretation of the situation. To test this anlyses using identical assay procedures of repeated extracts of tissue in (a) water and (b) normal acetic acid were made. Water would extract a negligible amount of the bound fraction of each ion, while acetic acid and nitric acid would remove most or all of the bound ions. These results are discussed in Section 3.2a.

2.3. Electrical circuit for Potential measurement.

The membrane potentials were measured across the plasmalemma and tonoplast with reversible electrodes. The electrodes used were two silver

chloride coated silver wires inserted into two 3M KCl salt bridges. The smaller of these salt bridges, the microelectrode, was inserted into the plant cell and the potential between this and the larger salt bridge, the reference electrode, in the external solution bathing the plant cell was recorded. An electrometer, with a high input resistance of about 10^{17} ohms, was selected as such a high resistance causes little drain of the current from the plant cell during measurement. The circuit employed is shown diagramatically in Figure 2.A. The potential measured was in fact the "resting potential" of the cell and there was no sign of any action potential under any circumstances.

An external backing-off circuit was employed to back the electrometer, millivolt meter, to zero after both electrodes had been placed in the solution bathing the plant cells. The millivolt meter usually registered a negative potential difference when both electrodes were

Figure 2A (Opposite).

DIAGRAMMATIC REPRESENTATION OF ELECTRICAL CIRCUIT USED IN CELL MEMBRANE POTENTIAL MEASUREMENTS.

A : Crocodile clip.

B : Reference electrode in drainage tube.

C : Perspex microscope stage with a channel round the edge.

D : Drainage tube.

E : Solution delivery tube.

F : Plant tissue under coverslip on microscope slide.

G : Microelectrode held in chuck of micro-manipulator.

H : Spring clip.

L : Backing off circuit.

K : High impedence mV meter.

M : Audio signaller.

FIGURE 2A

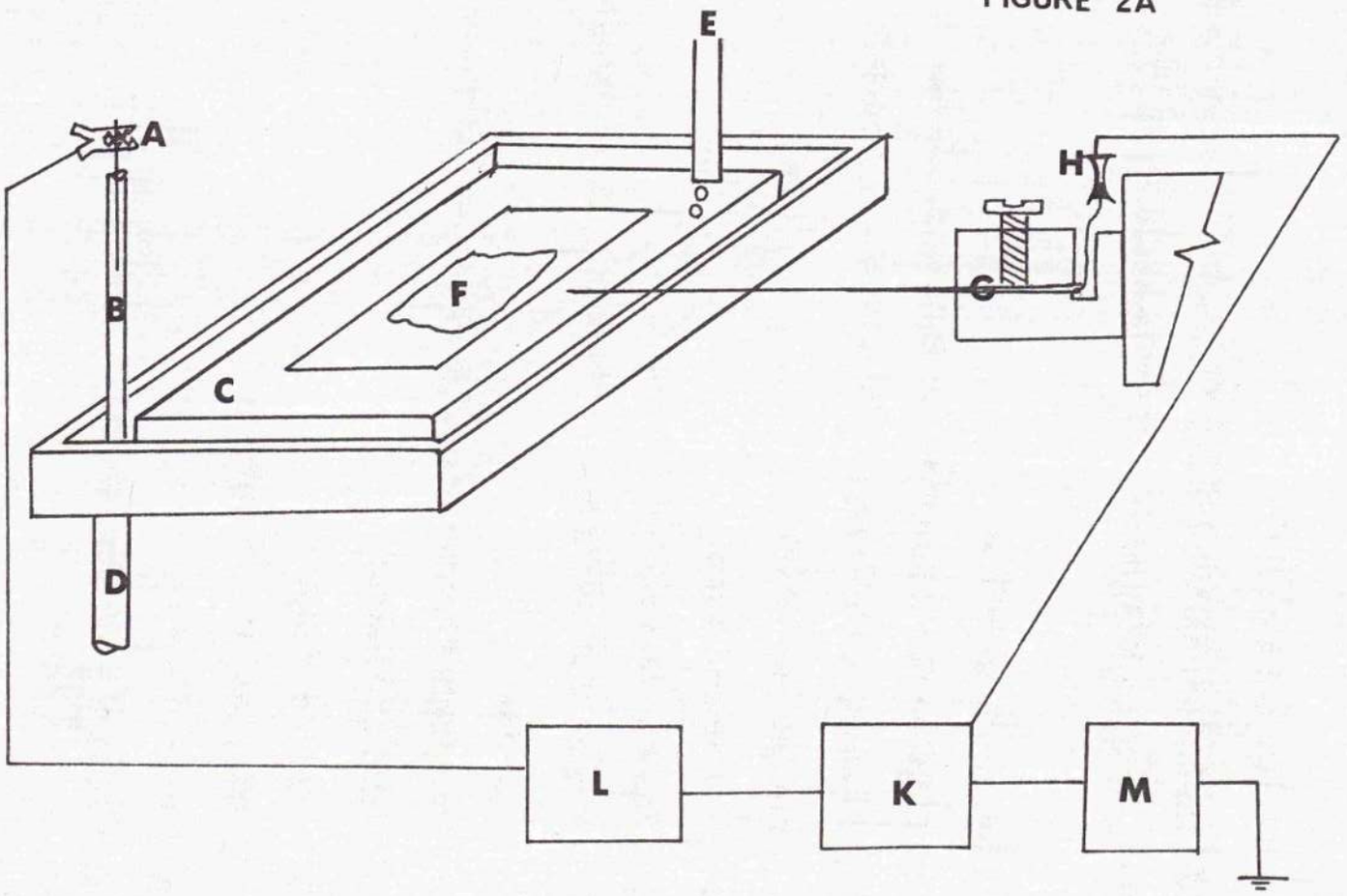

placed in the bathing solution due to tip potential. An audio signal analog unit was driven from the recorder output of the electrometer the frequency of the signal increasing as the reading on the millivolt meter became more negative. This enabled the operator to "hear" the e.m.f. being measured without looking up from the microscope during adjustments.

2.4. Tip Potentials.

Tip potentials arise across the interface of the 3M KCl solution in the tubular tip of the electrode and the bathing solution. The movement of any ion across this interface causes a potential. K and Cl ions have similar mobilities and the movement of ions of similar mobilities across an interface reduces the potential well below the value expected if both ions were to move at differing rates. The presence of a zeta potential along the inner walls of the microelectrode tubing, which due to the narrow tip of the tube is greatly increased

in the tip area, tends to reduce the mobility of the ions of opposite charge to this potential, namely Cl. Thus K is more free to diffuse rapidly from the tip causing a tip potential. The ions diffusing into the tip from the solution, mainly Na, also contribute to the tip potential.

The tip potential was backed off to zero in the bathing solution before the micro-electrode was placed in the plant cell. Due to the different ionic composition of the external solution and the cytoplasm and vacuolar content of the cell a new and different tip potential could arise. This would be additive to the actual cell membrane potential, so the actual cell membrane potential would be different to the one recorded. In theory this could be over-come by backing off the tip potential in a solution with the same ionic concentrations as the cytoplasm and the vacuole. This was im-possible in E. intestinalis where these were not known separately. The differences in the tip potentials in sea water and intracellular

ion solutions would, however, be quite small. The differences in tip potentials at the high salt concentrations employed were therefore assumed to be minimal.

2.5. Making of Electrodes.

Two inch microelectrodes were made from 7740 Corning Glass tubing which was melted and pulled in a vertical traction device built at the Gatty Marine Laboratory. The tubing was heated around its central region by a tungsten coil as the two ends of the tube were pulled apart. This vertical device has the advantage over pullers that work in the horizontal in that the tip of the electrodes are straight and not curved due to gravitational forces on the molten glass.

The electrodes were filled, tip downwards, with methanol under reduced pressure, and transferred to distilled water and finally to 3M KCl 56 hours before use. The size of the

electrode tip required is governed by at least two factors, the tip must be small enough to penetrate the cell wall, cytoplasm and vacuole without damaging the cell and the electrical tip resistance must not be too low. Only electrodes having a tip resistance from 50 to 150 Mohms were used which corresponds to an internal tip diameter of about 0.10 um. which was confirmed by direct electron microscopic observation. (M.G. Stanton, personal communication)

In order to reduce the streaming potentials that may occur when a small diameter electrode is placed in a flowing solution, reference electrodes were made from 7cm. lengths of 0.4cm. diameter glass tubing and were filled with 3M KCl in agar gel and placed in the outflow to prevent contamination of the medium flowing over the cells themselves.

2.6. Potential Measurements.

Measurements of cell membrane potentials

were made on illuminated tissue under the high power of a microscope which was attached to a microelectrode manipulator. This device was designed at the Gatty Marine Laboratory and allows the microelectrode tip to be positioned with an accuracy of within 1um., and has no back lash or run on.

The potential recorded when the microelectrode was placed in the bathing solution, the tip potential, was "backed off" to zero before the penetration of the cell was begun. The difference between the tip potential in sea water and intracellular solutions was assumed to be minimal at the high salt concentrations prevailing. Only voltages which remained steady for more than one minute were recorded. The membrane potential across the plasmalemma between sea water and the cytoplasm was measured after driving the microelectrode into the cytoplasm parallel to and close beside the cell wall; chloroplasts could be seen to be displaced by

the advancing tip. Placing the electrode tip in the vacuole was more difficult; evidence indicates that this was achieved. The fine microelectrode tip was driven at a slow steady rate without elastic back lash through the centre of the wall across the cytoplasmic lining and into the vacuole of a cell sited one or more cells in from the edge of the piece of tissue. Since the cell being penetrated was supported by the turgor of its neighbours, dimpling of the cell before penetration was minimal; thus upon penetration the tip did not spring forward into the layer of cytoplasm on the further side. Controlled and rapid siting of the tip was thus possible. Cytoplasmic streaming has not been observed in these cells, so that rapid cytoplasmic sealing over an electrode tip in the vacuole is unlikely.

Two distinct potentials were never observed within a single cell either upon steady penetration through the cytoplasm and vacuole or

upon slow withdrawal of the microelectrode. For comparison large voltages across the tonoplast have regularly been observed in some other plant cells using the same method and apparatus.

2.7. Flux Measurements.

Influx and efflux rates for each ion were calculated from measurements of exchanges of radioactive tracer ions between illuminated tissue and solutions at 20°C. (except in low temperature or darkness exchange experiments). For both influx and efflux measurements the tissue was counted and not the relevant bathing solution. Tissue counting gave more accurate results when for experimental reasons the ratio of volume of bathing solution to tissue was large and only small changes of tracer content occurred in the bathing solution.

Efflux measurements; pieces of uniform tissue, (see Section 2.1), were removed from the

equilibrating solution and blotted free of any surface solution. These pieces were then immersed in the "loading" solution containing the radioactive tracer ion to equilibrate isotopically for at least 24 hours. After equilibration each piece of tissue was removed from the tracer solution and shaken free of surface liquid. Each piece of tissue was then placed into a separate $20cm^3$ container of stirred tracer-free solution for different periods of time, during which the radio nuclide moved from the cells into the medium. A large volume of bathing solution was used to reduce re-entry of tracer to the tissue from the bathing solution during long eluting periods. The ratio of volume of tissue to solution was such that the eluted radioactive tracer concentration in the bathing solution was in all cases immeasurably low; re-entry of the radio isotope into the tissue was therefore negligible. Efflux measurements were continued until the tissue counts could no longer be distinguished

above background level.

On removal from the solution the tissue was blotted by placing between two sheets of soft absorbent paper and a standard weight of 52g. was rolled once over the tissue, (see Appendix 2). Any remaining liquid film was negligible and therefore any radioactivity remaining on the thallus was negligible. The tissue was then placed flat on a planchet which had been smeared with egg albumen and placed on a hot plate to dry. Thus the geometry of counting could be interpreted with weak beta emitters such as Cl.

Influx measurements; comparable pieces of uniform tissue were blotted and immersed separately for different periods of time in a solution containing the radioactive tracer, after which they were removed and blotted for counting as above. Influx measurements were continued until the tissue counts rose to and remained at a constant maximal value for more than 24 hours.

2.8. Calculation of Flux Rates.

It will be shown below that the influx of all tracers into the cell consists of two phases, an initial rapid phase, which is uptake into the cell walls, and a second slower phase which is uptake into the intracellular protoplast volume or apparent osmotic volume (A.O.V.) of the cell. This pattern of exchange was also obtained with tracer effluxes. The one phase exchange of the A.O.V. allows membrane fluxes to be calculated by the methods discussed below.

The model used for the interpretation and calculation of flux rates has been selected because it is the simplest model based upon the minimum number of assumptions. This approach has been widely used by other workers amongst them MacRobbie (1962) and West and Pitman (1967). It is assumed that the efflux rate is a function of intracellular content. A linear plot of $\ln \left(\frac{Q^{*}max. - Q^{*}}{Q^{*}max.}\right)$ against time would be predicted by this model, where Q^{*} is the tracer content of the tissue at any instant and $Q^{*}max.$ is the maximal tracer content of the tissue. In Enteromorpha intestinalis the use of

Figure 2B (Opposite).

Figure 2B shows a logarithmic plot of ($Q^{*}max-Q^{*}$) against time in minutes for Cl (•) and Na (○). Where Q^{*} is the total tracer ion content in the tissue at any instant and $Q^{*}max$ is the maximal tracer ion content of the tissue.

FIGURE 2B

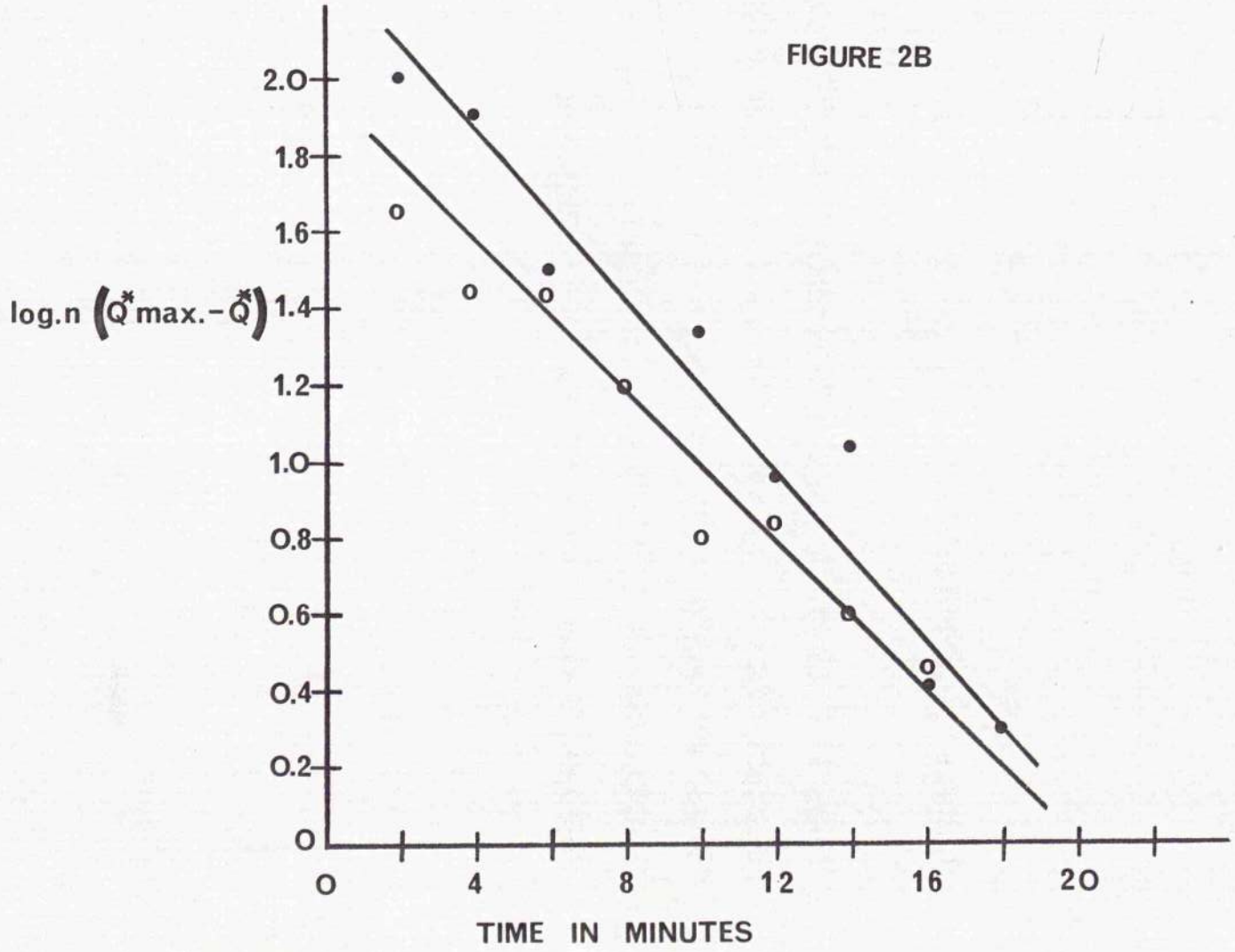
log.n (Q*max.-Q*)
2.0
1.8
1.6
1.4
1.2
1.0
0.8
0.6
0.4
0.2
0
0
4
8
12
16
20
TIME IN MINUTES

Figure 2C (Opposite).

Figure 2C shows a logarithmic plot of ($Q^{*}max-Q^{*}$) against time in minutes fro K. Where Q^{*} is the total tracer ion content in the tissue at any instant and $Q^{*}max$ is the maximal tracer ion content of the tissue.

FIGURE 2C

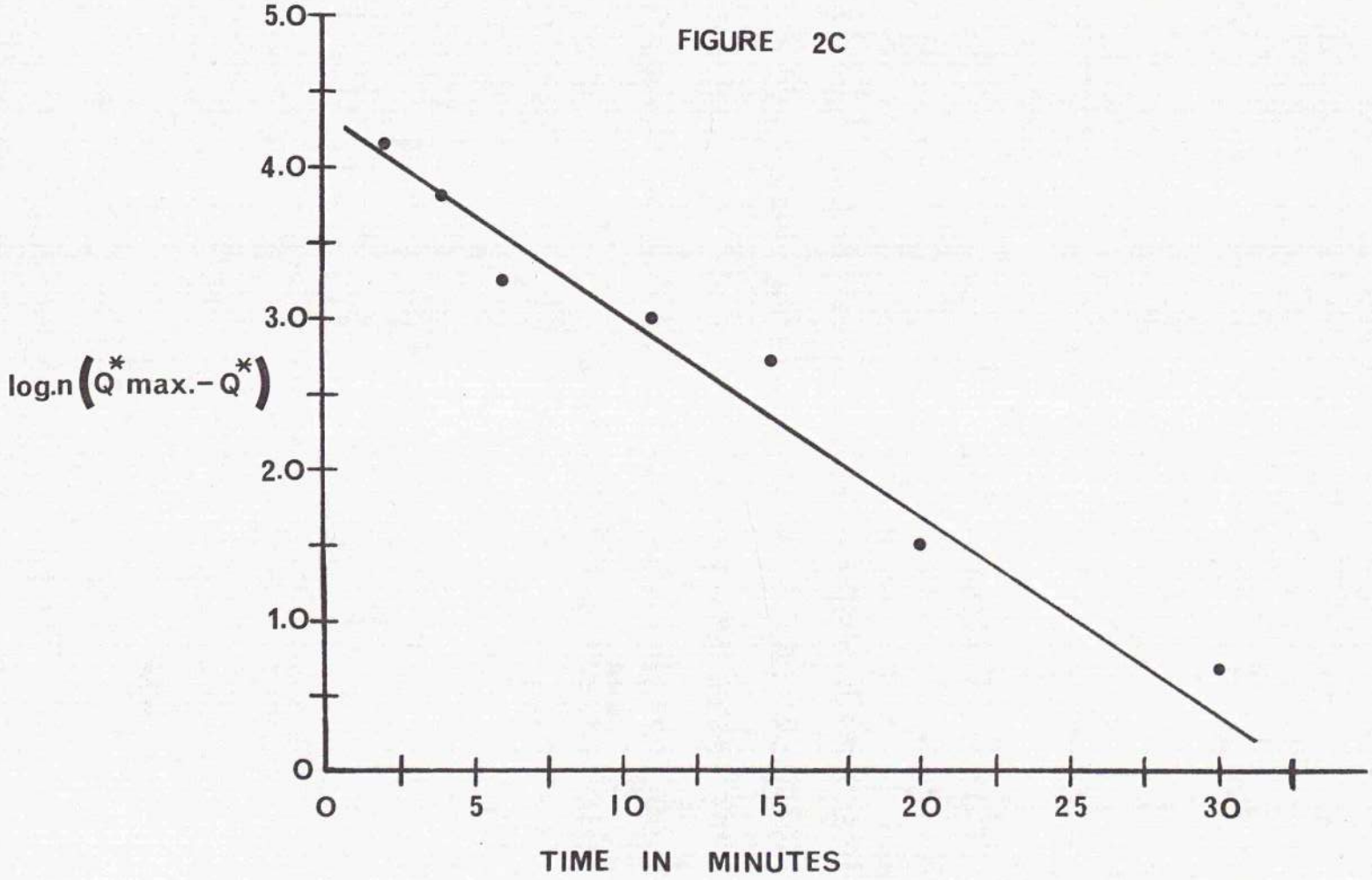

such a model is supported by the fact that such plots are linear. (Graphs of $\ln \frac{(Q^*_{max.} - Q^*)}{Q^*_{max.}}$ are not in fact shown since graphs of $\ln (Q^*_{max.} - Q^*)$ against time (Figures 2B and 2C) have been plotted and are linear, therefore $\ln \frac{(Q^*_{max.} - Q^*)}{Q^*_{max.}}$ will be linear as Q max. is a constant.) An alternative assumption that intracellular ion content and efflux are independent, which does not apply in E. intestinalis, has been fully discussed by Saddler (1970).

The efflux rate J_{io} for each ion is calculated from the rate of loss of tissue tracer into inactive solution. The rate of tracer loss and the tracer content in the tissue both decrease exponentially with time. The decrease in rate of loss of tracer from the tissue is caused by the fall in total tracer content within the tissue with time. The rate of efflux J_{io} can most simply then be related to the total tracer content Q in the tissue at any instant

and also to the total concentration Q of that ion in the tissue; it can be shown that, for each kind of ion in turn,

$$J_{io} = - \frac{dQ^*/dt}{Q^*/Q} \quad - - - \quad 2.1$$

Influx rate J_{oi} is similarly calculated; the rate of tracer uptake, which at any instant is assumed to be a function of (Q max. - Q) is given by

$$J_{oi} = \frac{dQ^*/dt}{(Q^*max. - Q)/Q} \quad - - - \quad 2.2$$

where Q max. is the maximal tracer content of the tissue after prolonged exposure to labelled solution. Graphs of ln (Q^* max. - Q^*) against time are linear and indicate that the values of Q^* max. used in the calculations are correct, (Figures 2B and 2C).

2.9. Calculation of Passive Permeabilities.

Passive permeability values of K, Na and Cl in the various experimental solutions have been calculated by applying data for cell

membrane potential, ion concentration and passive ion flux (along the electrochemical potential gradient) to the appropriate Goldman flux equation 2.3 or 2.4:

$$J_{oi} = - P_j \frac{ZFE}{RT} \frac{Co}{1-\exp(ZFE/RT)} \quad - - - \quad 2.3$$

$$J_{io} = + P_j \, ZFE \, \frac{Ci \exp(ZFE/RT)}{1-\exp(ZFE/RT)} \quad - - - \quad 2.4$$

where P_j = Passive permeability of ion

Z = Algebraic valence

F = Faraday

E = Measured cell membrane potential

R = Gas constant

T = Temperature degrees Kelvin

Ci = Internal concentration

Co = External concentration

J_{oi} = Influx

J_{io} = Efflux

A knowledge of the passive permeability P_j then allowed the expected passive flux in the opposite direction to the flux employed above, i.e. in the active direction, to be

calculated from the other flux equation. Assumptions implicit in this simple approach are discussed below.

2.10 Counting.

A Panax windowless scintillation counter was used to count the radioactivity in the tissue on the planchets. After counting each planchet three times the thallus was washed off the planchet, dried, and weighed. The mean of three counts was obtained for each piece of tissue and was then corrected to counts per minute per gram original fresh weight (c.p.m. g^{-1}.). Each count recorded was at least ten times the background. A correction was made to each count for ^{42}K to allow for the short half life of the isotope. Absorption of radiation within the dry tissue, which was about 4um. thick, was small and constant throughout each experiment.

2.11. Radioactive Solutions.

Radioactive ^{42}K, ^{22}Na and ^{36}Cl were used separately in the form of tracer NaCl or KCl at final activities of about 0.05 µCi/20ml. The specific activity of each solution was measured by the removal of 100 µl. aliquots which were spread on planchets, dried and counted.

2.12. Cell Surface Area Measurement.

Measurements of plasmalemma surface area per gram of tissue were made using a light microscope. A mean value of 3900 ± 120 cm^2g^{-1} was obtained and is in the range obtained for Ulva (West and Pitman, 1967). Microscopic measurements on 50 cells gave a mean relative volume of cytoplasm and vacuole as 39% ± 2.5% and 61% ± 3.0% repectively of the total protoplast volume, the protoplast being almost cylindrical, averaging 8 times 16 um. across, and occupying 0.61 ± 0.06 cm^3/g. of the whole living

tissue, the rest (0.40 ± 0.02 $cm^3/g.$) being thick cell wall. Results are given with standard errors as calculated in Appendix 1.

3. MEASUREMENT OF FLUX RATES, IONIC CONCENTRATIONS AND CELL MEMBRANE POTENTIAL IN SEA WATER.

3.1. Introduction.

The study of ionic relationships in plant cells is dependent upon measurements of the cell membrane potentials, their internal and external concentrations of the major ions and their partial fluxes. Such measurements in conditions of osmotic equilibrium may then be initially interpreted on a simple electrochemical basis. These measurements are reported in this section for *E. intestinalis* in sea water in which it had been grown. Evidence is presented for the active transport of all three major ions K, Na and Cl. Estimates of their passive permeabilities have been used to account for the observed cell membrane potential. This gives the basic ionic relationships in *E. intestinalis* in sea water.

3.2. Results.

3.2a. Analyses.

Nitric acid, acetic acid and distilled water were all used as media for refluxing plant material. Nitric acid, however, appeared to cause the release of ions bound to the cell wall into the solution, thus causing an ion concentration higher than actually present in the cell wall free space of the tissue, in sea water, to be recorded. Acetic acid and water were both used in separate analyses of plant material and the three sets of results compared, (Table 3i). As the results show, although the ion concentrations in the cell wall varied when different refluxing solutions were used the ion concentrations in the protoplast were more or less constant. As the ion concentrations in the protoplast were of more concern than those in the cell wall, and as nitric acid analysis

gave more consistent results on repeated analyses it was decided to use nitric acid only in subsequent analyses. The results obtained from nitric acid are therefore those which are used in calculations and discussions.

The concentrations of ions in the protoplast of the cell were calculated using a protoplast volume of 0.61 $\pm$ 0.06 $cm^3/g.$ tissue. This value was obtained by light microscope measurements and agrees closely with the values obtained from labelled mannitol experiments, (see Appendix 3). These results agreed closely with the concentrations predicted from isotope tracer experiments, assuming the same volume of (Table 3ii), calculated as shown in Appendix 1.

TABLE 3(i).

Comparison of cell wall and protoplasmic ion concentrations using different refluxing solutions.

Ion	Measured Cell Wall Content	Protoplast Content
	Analysis with Nitric Acid	
K	1342 ± 40	450 ± 21
Cl	1632 ± 64	370 ± 25
Na	2160 ± 93	260 ± 29
	Analysis with Distilled Water	
K	1180 ± 109	432 ± 53
Cl	678 ± 120	364 ± 53
Na	941 ± 111	276 ± 54
	Analysis with Acetic Acid	
K	1262 ± 56	459 ± 35
Cl	1402 ± 59	371 ± 40
Na	1792 ± 154	260 ± 60

Concentrations in milliMoles/litre.

All figures mean of 12 samples.

TABLE 3(ii).

Analysis of ion concentrations from tracer measurements during ion flux measurements.

Ion flux	Measured Cell Wall Content	Measured Protoplast Content
K influx	1504 ± 84	450 ± 14.0
K efflux	1047 ± 98	451 ± 14.7
Cl influx	1403 ± 47	328 ± 24.0
Cl efflux	2093 ± 91	360 ± 22.0
Na influx	2109 ± 86	271 ± 30.0
Na efflux	2106 ± 72	260 ± 33.0

Concentrations expressed in mM/l.

All figures mean of 6 samples.

3.2b. Fluxes.

Typical time courses of tracer ion fluxes are shown in Figures 3, A, B, C, D, E, and F. A logarithmic efflux time course for all three ions showed only two separate phases, the first rapid and the second slower although measurements were continued until no tracer was detectable in the tissue. Only an initial rapid phase of tracer uptake was obtained for each tracer ion when cell walls alone were used in place of living tissue, (Figure 3G). Dainty and Hope,(1959), had shown a similar effect in Chara australis. This indicated that the initial phase of tracer exchange was with the cell wall free space. The second slower phase was therefore considered to be tracer exchange with a non free space, or osmotic volume, of the cells which acted as a single kinetic compartment. In confirmation of this, rapid first phase was unaltered and only the second slower phase changed when the cells were

Figure 3A (Opposite).

Efflux of tracer Cl from E. intestinalis cells in non-radioactive sea water in the light at 20°C. Each point is the mean of 6 samples with standard error of the mean shown by a vertical line.

FIGURE 3A

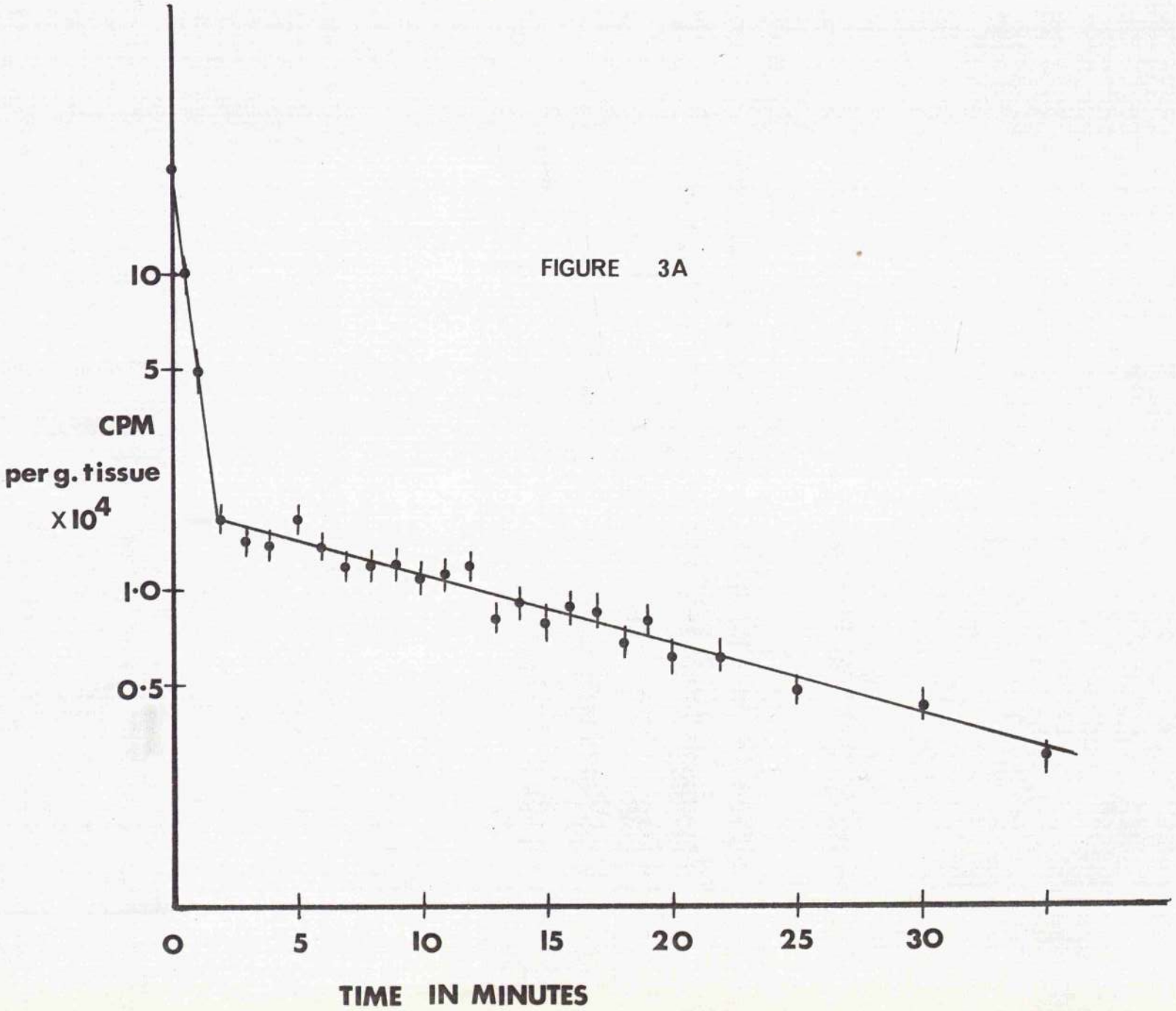

Figure 3B (Opposite).

Uptake of Cl^{36} from sea water by E. intestinalis in the light at 20°C. Each point is the mean of 6 samples with standard error of mean shown by a vertical line.

FIGURE 3B

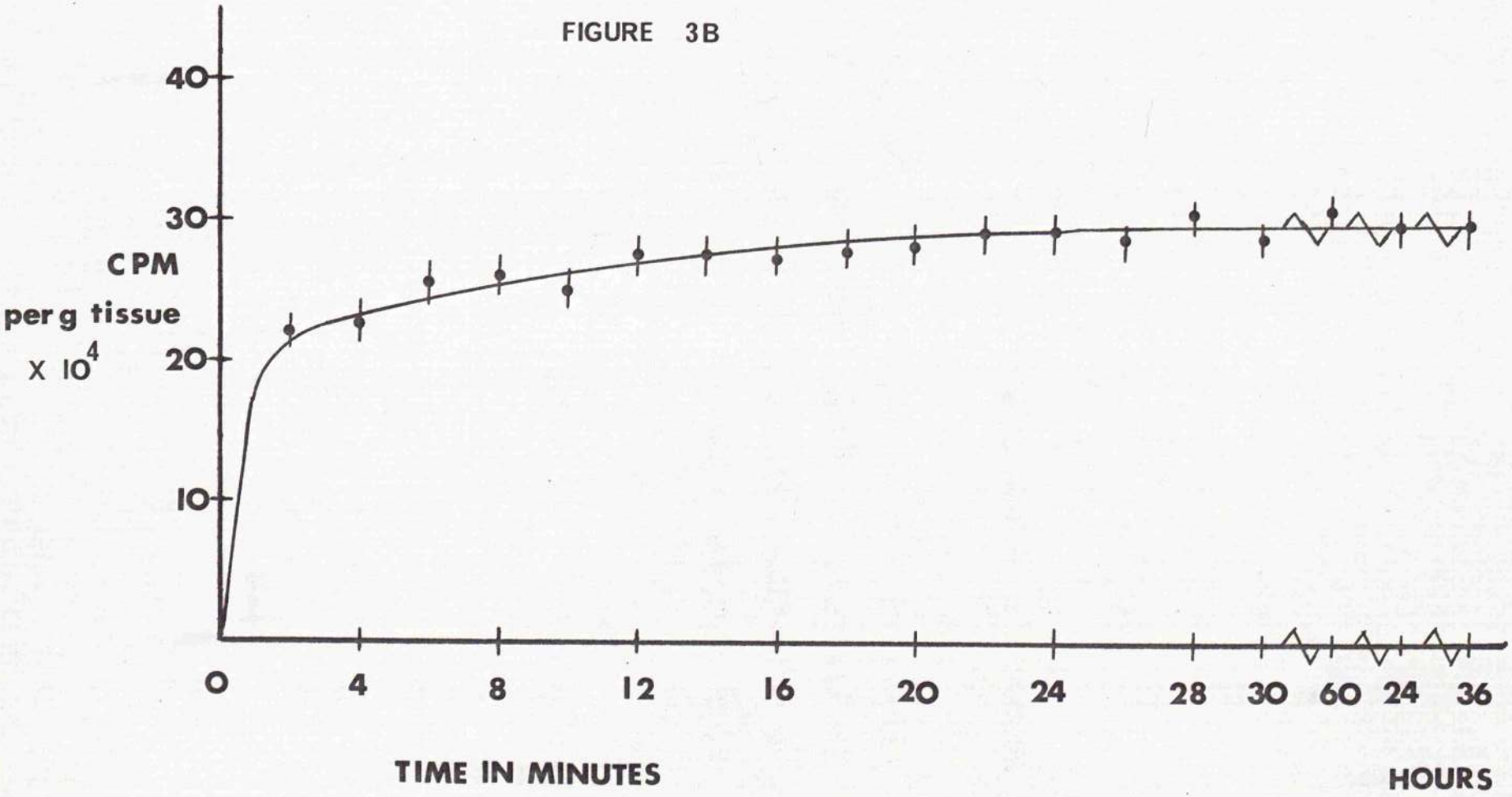
40
30
CPM
per g tissue
X 10^4
20
10
0
4
8
12
16
20
24
28
30
60
24
36
TIME IN MINUTES
HOURS

Figure 3C (Opposite).

Efflux of tracer ^{42}K ions from E. intestinalis cells into non-radioactive sea water in the light at 20°C. Each point is the mean of 6 samples with standard error of mean shown by a vertical line.

FIGURE 3C

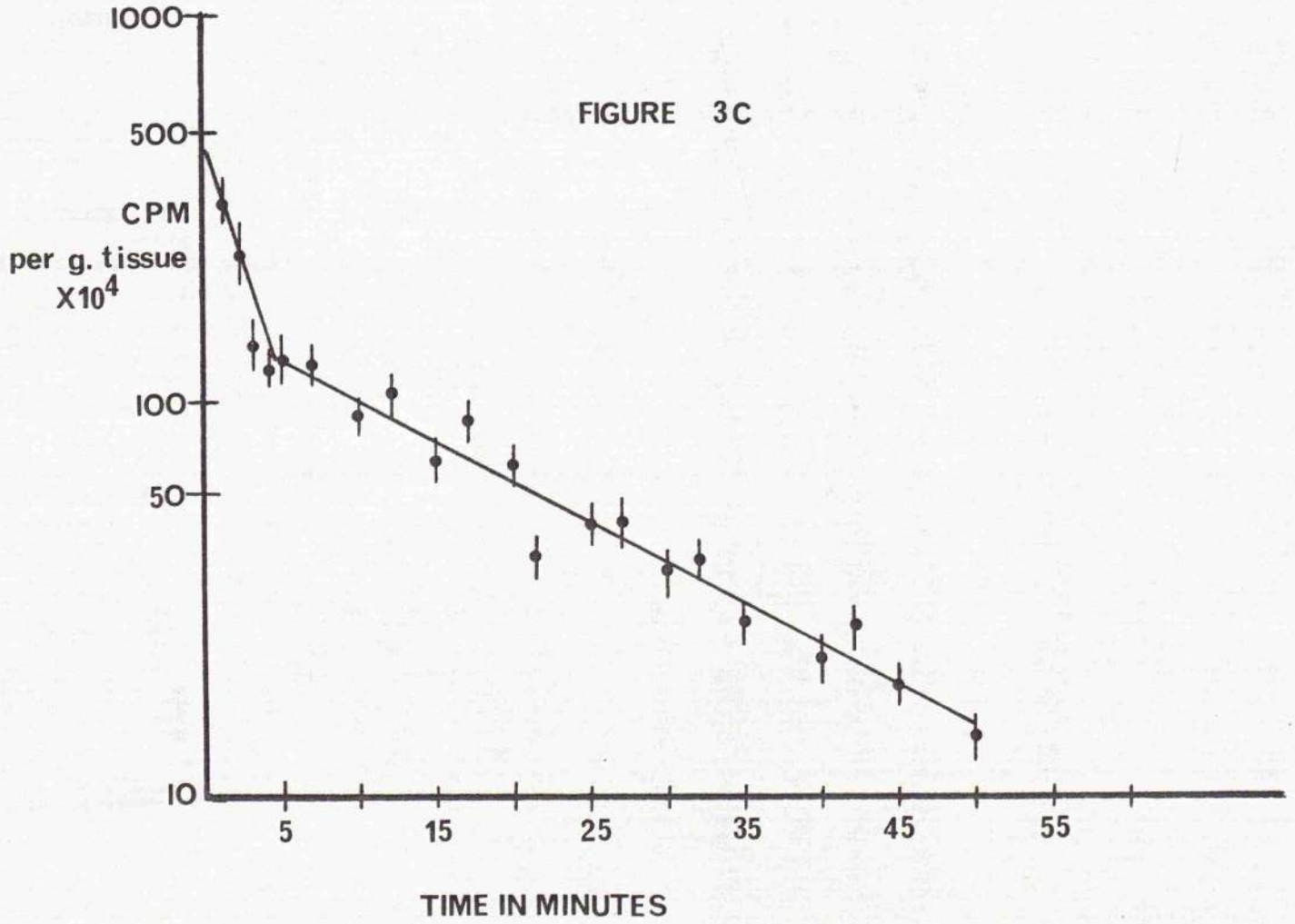
1000
500
CPM
per g. tissue
X10^4
100
50
10
5
15
25
35
45
55
TIME IN MINUTES

Figure 3D (Opposite).

Uptake of ^{42}K from sea water by E. intestinalis in the light at 20°C. Each point is the mean of 6 samples with the standard error of the mean shown by a vertical line.

FIGURE 3D

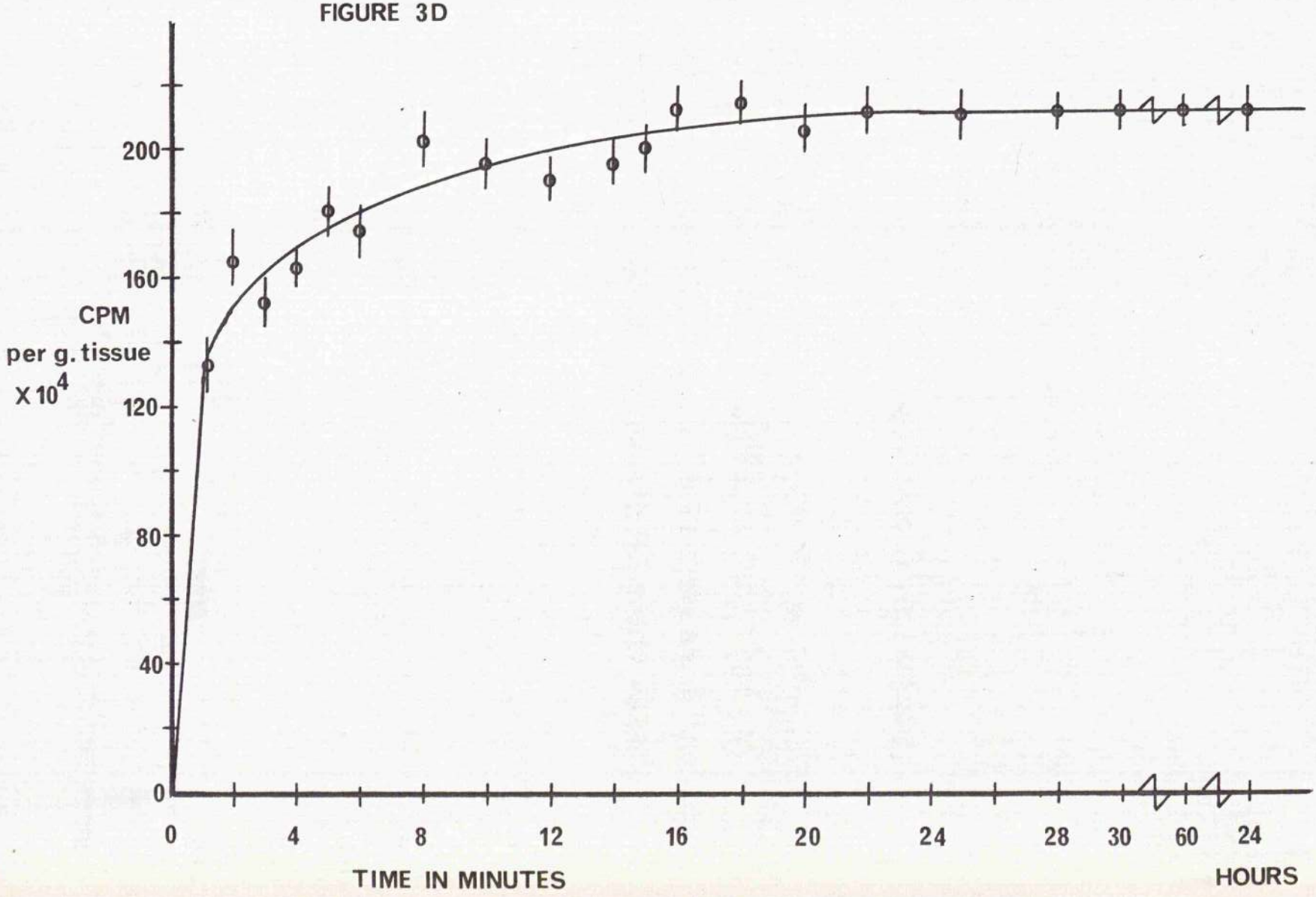
CPM
per g. tissue
X 10^4
200
160
120
80
40
0
0
4
8
12
16
20
24
28
30
60
24
TIME IN MINUTES
HOURS

Figure 3E (Opposite).

Uptake of ^{22}Na from sea water by E. intestinalis in the light at 20°C. Each point is the mean of 6 samples with standard error of mean shown by a vertical line.

FIGURE 3E

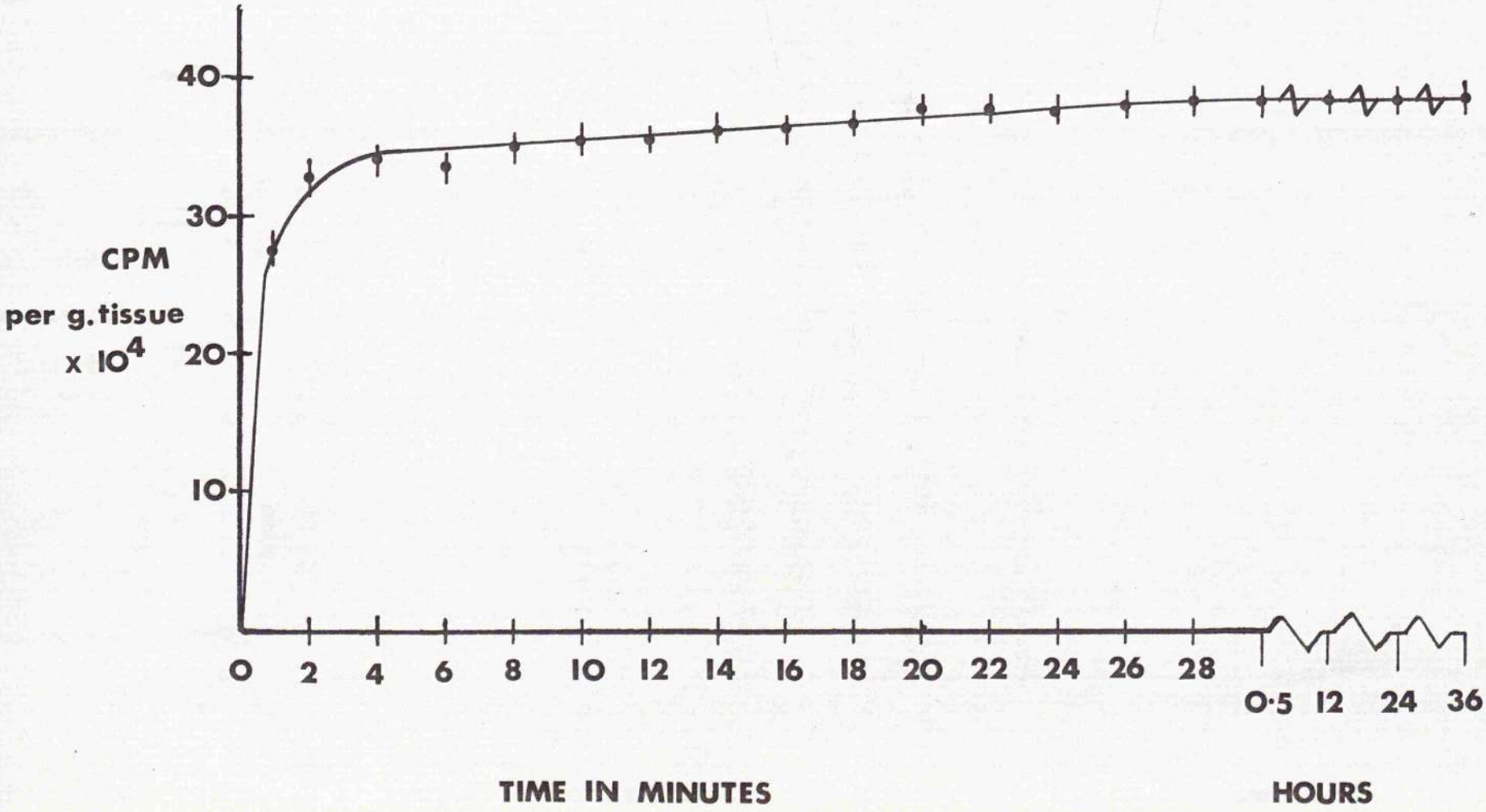
40
30
20
10
CPM
per g. tissue
x 10^4
0
2
4
6
8
10
12
14
16
18
20
22
24
26
28
0·5
12
24
36
TIME IN MINUTES
HOURS

Figure 3F (Opposite).

Efflux of tracer ^{22}Na ions from *E. intestinalis* cells into non-radioactive sea water in the light at 20°C. Each point is the mean of 6 samples with standard error of mean shown by a vertical line.

FIGURE 3F

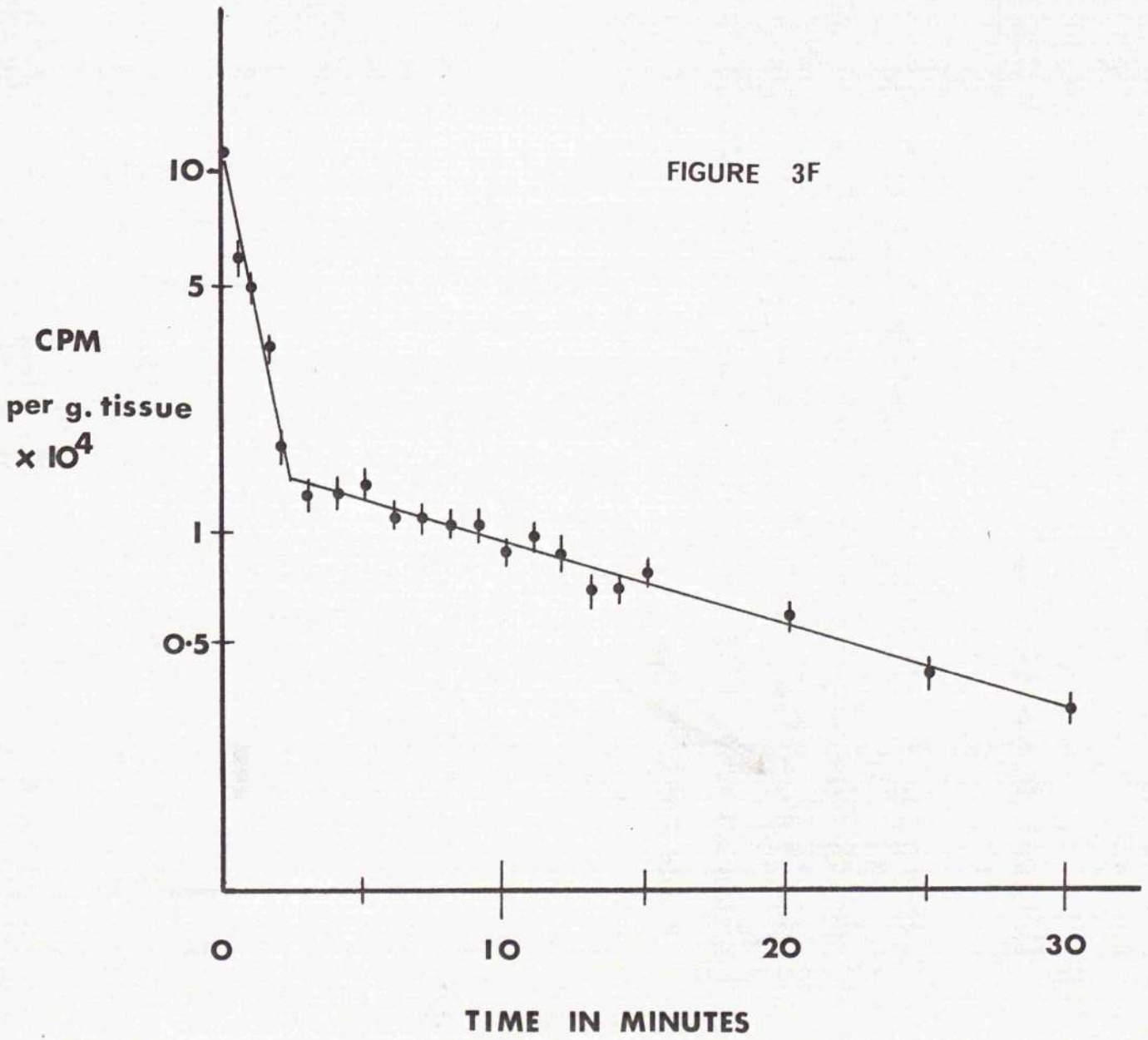

Figure 3G (Opposite).

Efflux of tracer ^{42}K ions from cell walls alone of E. intestinalis into non-radioactive sea water in the light at 20°C. Similar results were obtained for ^{36}Cl and ^{22}Na (not shown). The efflux was followed until counts could not be distinguished above background level. Each point is the mean of 6 samples with the standard error of the mean shown by a vertical line.

FIGURE 3G

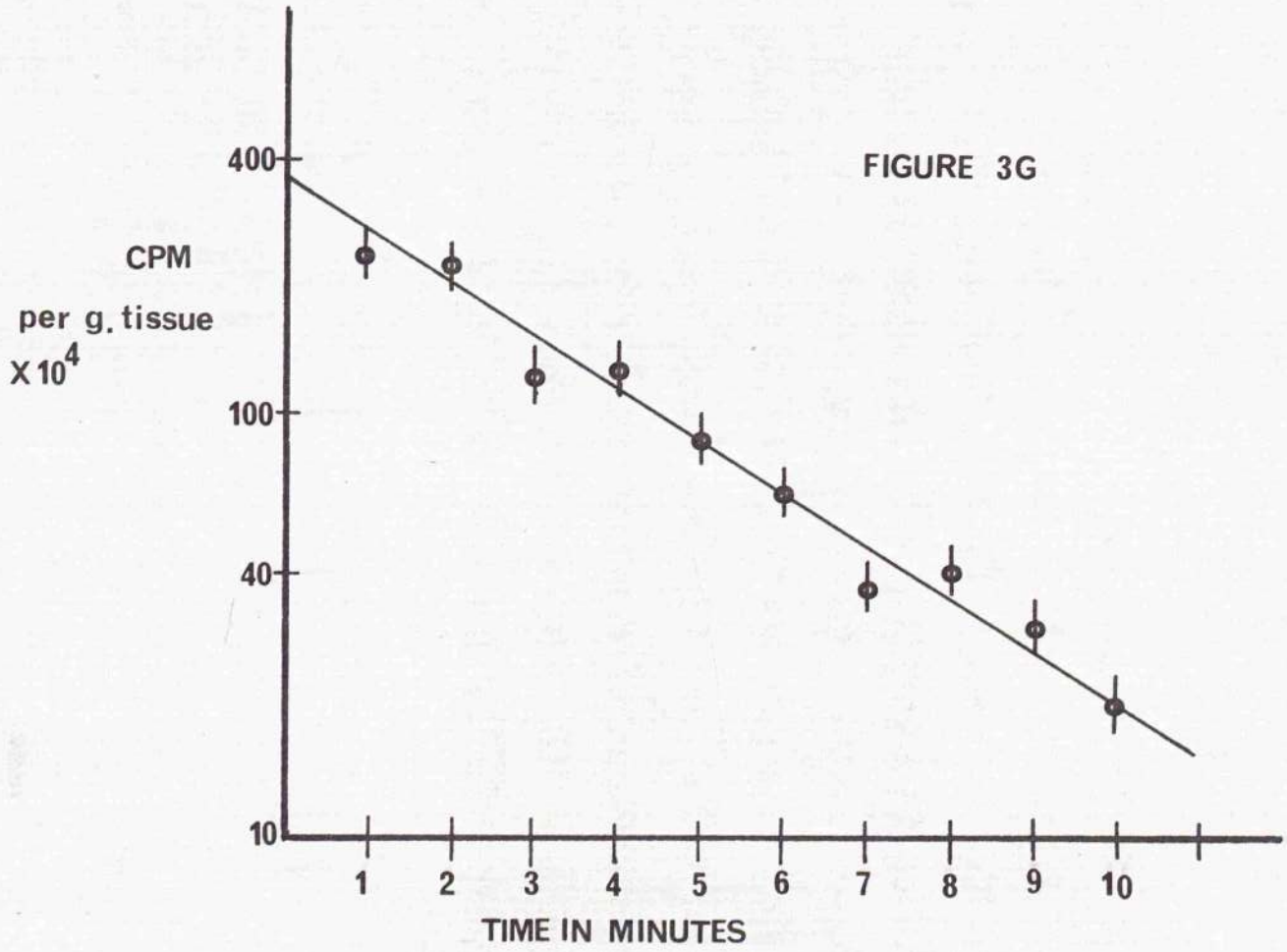
CPM
per g. tissue
X 10^4
400
100
40
10
1
2
3
4
5
6
7
8
9
10
TIME IN MINUTES

darkened, cooled or exposed to metabolic inhibitors. These treatments did not alter the rapid tracer exchange of the cell walls alone. Hence data from the second slower kinetic phase alone have been used for calculating membrane fluxes, (Table 3(iv)).

3.2c. Cell membrane potential.

The mean membrane potential across the plasmalemma of 50 cells between the interior of the protoplasm and sea water was -42 ± 1.5 mV. Membrane potential between the sea water and either vacuole or cytoplasm was the same i.e. there was no evidence for a significant voltage across the tonoplast.

3.2d. Ion concentratios and potentials.

These are shown in Table 3(iii). The assumptions used in calculating internal concentrations have been discussed above.

TABLE 3(iii).

Ion concentrations and cell membrane potentials in sea water in the light at 20°C.

Ion	External Concentration mM/l	Internal Concentration mM/l	Measured EMF, E_m. mV(1)	Calculated EMF, E_j. mV(2)	ΔE ($E_m - E_j$) mV(3)
K	11	450 ± 5.6	-42 ± 1.5	-97.4	+55.4
Na	460	260 ± 1.5	-42 ± 1.5	+18.6	-60.6
Cl	560	370 ± 4.1	-42 ± 1.5	+4.0	-46.0

(1) E_m is the measured cell membrane potential.

(2) E_j is the EMF calculated assuming passive transport of ions across the cell membrane, using the Ussing-Teorell equation (1.1).

(3) Δ E is the difference between E_m and E_j.

Standard errors are quoted for 50 measurements of cell membrane potentials and for 12 measurements of concentrations.

A sample calculation of E_j is shown in Appendix 1.

TABLE 3(iv).

Ion flux rates between cells of E. intestinalis and seawater in the light.

Ion	Influx	Efflux
	picomoles cm^{-2} sec^{-1}	
Na	37.8 ± 2.2	43.9 ± 2.7
K	91.5 ± 5.6	81.1 ± 5.1
Cl	68.3 ± 4.0	54.9 ± 3.0

Cells in white light at 20°C. Fluxes calculated as described under Methods (Section 2.8). Standard errors are quoted for 6 replicates in each case.

A sample calculation of flux rate is given in Appendix 1.

Figure 4A (Opposite).

The rate of Na efflux in the light at 20°C plotted against external K concentration. Each point is the mean of 6 samples with the standard error of the mean shown by a vertical line.

FIGURE 4A

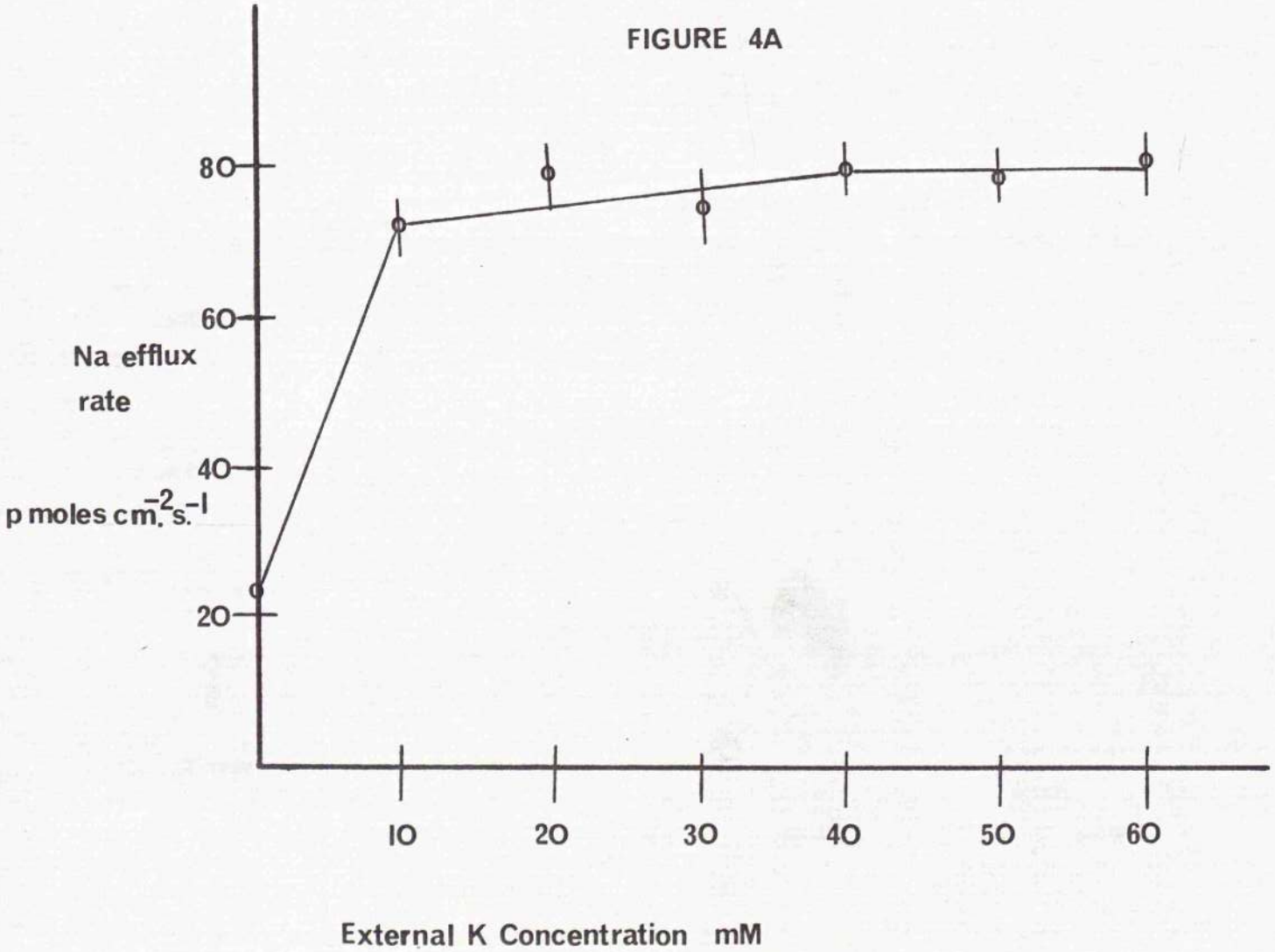
80
60
40
20
Na efflux
rate
p moles cm.$^{-2}$s.$^{-1}$
10
20
30
40
50
60
External K Concentration mM

3.3. DISCUSSION.

The value of the membrane potential of *E. intestinalis* is small compared with that of most other algae, although Gutknecht and Dainty, (1968), site a potential of -42 mV across the plasmalemma of *Porphyra* in sea water. Dodd, Pitman and West, (1966), report a potential of -35 mV across the plasmalemma of *Chaetomorpha*. The small membrane potential of *E. intestinalis* in sea water may be connected with the plant's ability to inhabit tidal regions and fresh water where the cell membrane potential can be more than 100% greater.

From the tracer influx and efflux curves, there appears to be only one phase for intracellular osmotic volume exchange, (see Section 3.2b.). Since the whole membrane potential of -42 mV occured across the plasmalemma, it is assumed that the intracellular osmotic volume includes the cytoplasm as in other cells studied.

There was no measurable potential difference across the tonoplast.

Since the cytoplasm, including chloroplasts, and the vacuole are kinetically indistinguishable and similar in volume it could be assumed that either the plasmalemma fluxes are much more rate limiting than those across the tonoplast or plastid membranes; or that the ion concentrations in the vacuoles and plastids are negligible compared with those in the cytoplasm.

The small size of the cell prevents chemical analysis of the ionic content of the vacuole and cytoplasm separately; the single phase kinetics does not allow estimation of their separate ionic contents. If we assume that the ions are distributed between both cytoplasm and vacuole, it is possible to calculate the volume of the protoplast occupied by tracer from knowledge of the tracer distribution at isotopic equilibrium and to compare

this with the actual protoplast volume measured microscopically.

$$\text{total counts in protoplasmic volume at isotopic equilibrium} = \frac{\text{number of mMoles total ion within protoplasmic volume}}{\text{specific activity of bathing solution.}} \quad 3.1.$$

The equation assumes that cytoplasm and vacuole are in approximate water potential equilibrium.

The volume that the calculated number of mMoles would have to occupy in order to give the ionic concentration measured by analysis and assumed to be in the protoplast volume can then be determined. The calculated protoplast volumes from Cl, Na and K data were 0.65cm^3/g, 0.66cm^3/g and 0.60cm^3/g respectively. The living protoplast volume measured by light microscopy was 0.61 ± 0.06 cm^3/g which is thus consistent with the assumption that these similar ions occur in both cytoplasm and vacuole. This would be expected on osmotic grounds if a balance of water potential and electric charge has to be maintained between the cytoplasm and vacuole. Thus each of the ions is probably distributed relatively equally between both cytoplasm and vacuole. This would lead to 3-phase efflux kinetics for each ion if their tonoplast fluxes were significantly lower than those across the plasmalemma. Since, however, only a single kinetic phase is found for the efflux of each ion

from the protoplast, it is concluded that the tonoplast fluxes are not rate-limiting and that all the fluxes being measured are those across the plasmalemma. The use of total internal ionic concentration for a particular ion to calculate E_j from the Ussing-Teorell equation is thus reasonably justified, especially as there appears to be very rapid equilibrium between cytoplasm, vacuole and plastids. Even the improbably extreme assumption that all these ions are in the vacuole alone would not alter the conclusions as to the existence and direction of the active fluxes.

The ion flux rates are relatively high when compared in units of picomoles cm^{-2} plasmalemma sec^{-1} with those of other algae. The comparatively high flux rates together with small cell size would mean that for E. intestinalis the internal ion content could be rapidly adjusted, whereas larger cells with equal membrane flux rates would take longer to

adjust whole cell ion content. The ability to adjust whole cell ion content rapidly would be of great ecological advantage to an estuarine alga. The passive permeabilities of K, Na and Cl have been calculated from the Goldman flux equations as discussed in Section 2.9. This approach assumes that the ions assort passively and independently. The permeability values are:- $P_{Na} = 40 \times 10^{-9}$, $P_K = 503 \times 10^{-9}$, $P_{Cl} = 72 \times 10^{-9}$ cm sec^{-1}. This gives a P_{Na}/P_K value of 0.080 which is similar to that of Chara australis (Hope and Walker, 1961) while P_{Cl} is higher than recorded for most other algae. The membrane potential is most affected by the passive K flux.

Assuming that the Goldman (Dainty, 1962) equation (1.2) is applicable to passive ion transport in cells of E. intestinalis one can predict the membrane potential $E_{Goldman}$ which would be generated by the passive diffusive fluxes of the three main component ions studied here. $E_{Goldman} = -42.8mV$, while the observed

E_m = -42 ± 1.5mV. Thus, passive diffusion of the three major ions alone probably determines the observed membrane potential in sea water.

For each ion a flux occurs in one direction against its electrochemical potential gradient. This flux for each ion must comprise two components, one a small diffusional passive flux and the other a larger flux due either to active transport or less probably to a coupled 1:1 exchange transport of that ion, the latter leading to isotope equilibration but no net flux. It has been shown in Sections 4 and 5 that the flux of each ion against its electrochemical potential gradient is decreased by one or more of darkening, cooling and application of inhibitors, while the flux along its electrochemical potential gradient is hardly or not affected. This is inconsistent with coupled influx-efflux exchange transport of each ion. Thus K and Cl must be actively transported into, and Na out from, the cells against the minimal

energy gradient given by the values ΔE (i.e. $E_m - E_j$) (Table 3(iii)). Each active transport system may tentatively be sited at the plasmalemma for the reasons discussed above. Absence of a measurable membrane potential across the tonoplast need not indicate the absence of active transport of ions across this membrane if the sum of the active and passive coupled ion transport cancels net charge flow. Since the rates of the putative active and passive ion flows can be differentially altered by darkening, cooling and application of inhibitors without producing a detectable membrane potential across the tonoplast (see Sections 4 and 5), rapid active transport at the tonoplast is unlikely.

If it is assumed that the tracer flux values are correct there is a net anion influx in the light of 9.1 picomoles cm^{-2} sec^{-1} across the plasmalemma. This would hyperpolarise the cells unless there was a balancing influx of some other cations e.g. Mg. The standard

errors of the mean flux rates are about 6, so that for illuminated cells the net flux may not significantly differ from zero. Such a rapid net continuing ion influx is improbable since it would require rapid cell growth which is not observed. However, the cells were illuminated for only 12 hours each day and it has been shown (Section 5) that this net anion influx does not occur in darkness. Since the experiments were conducted early in the light period it is possible that the observed net flux represents the daily movement towards flux equilibrium in the light. A similar disequilibrium is thought to occur after the beginning of the dark period when the light dependent components of the fluxes stop, (see Section 5). If there is such a cycle any such net flux would not then continue which is consistent with the observed long term constancy of the internal ionic concentration when this is measured at the same time of day.

4. EFFECTS OF TEMPERATURE, OUABAIN AND POTASSIUM CONCENTRATION ON SOME ION FLUX RATES.

4.1. Introduction.

In this section the effects upon influx and efflux rates of K, Cl and Na, of low temperature, ouabain, absence of certain ions from the medium and combinations of these treatments are reported. This enabled an attempt to partition various fluxes into active and passive components; the latter have been compared with those predicted on electrochemical grounds.

Lowering the temperature allowed some distinction between passive diffusional fluxes and those which were active and dependent upon metabolism or coupled to another active influx. Investigation has been made as to whether the coupling between components of the Na efflux and K influx involved an active transport system or could be through the membrane potential only.

4.2. Additional Methods.

4.2a. Solutions employed.

Ouabain was used routinely at a concentration of 0.5mM in sea water after this concentration had been shown to inhibit Na efflux maximally, (Table 4.(i)). The compositions of solutions used are shown in Table 4(ii) and are taken from Sverdrup, Johnson and Fleming (1942).

TABLE 4(i).

Effects of ouabain upon Na efflux from E. intestinalis in the light in seawater at 20°C.

Ouabain (mM)	Flux rate
0.0	42.7 ± 2.8
0.05	20.1 ± 1.9
0.50	12.2 ± 1.6
5.0	13.4 ± 1.8

Concentration of ouabain causing 50% of maximal inhibition is approximately 0.03mM. Flux rates in picomoles cm^{-2} sec^{-1}.

TABLE 4(ii).

Artificial solutions.

Ion	Control: as for seawater	No K
Na	470	470
K	10.0	0
Mg	53.4	53.4
Ca	10.0	10.0
Cl	548	538
SO_4	38.2	38.2

Concentrations in milliMoles per litre.

Solutions of varied K content: KCl added to No K solution in steps of 10 mM/l from 0 to 60.

4.3. Results.

4.3a. Cell membrane potential.

The mean cell membrane potential of at least 50 cells in each experimental solution in the light was determined between the interior of the protoplasm and the bathing solution. The results are given in Table 4(iii) below. There was no evidence for a significant voltage across the tonoplast in any solution.

TABLE 4(iii).

Cell membrane potentials recorded in different experimental solutions.

	Solutions	Cell membrane potential (mV)
A 20°C	Seawater	-42 ± 1.7
	Seawater + 0.5mM Ouabain	-42 ± 1.7
	Control + Ouabain	-44 ± 1.1
	Control	-44 ± 1.5
	Control - K	-52.1 ± 2.1
B +2°C	Seawater	-15 ± 1.4

4.3b. Fluxes.

All fluxes showed typical two-phase time courses and these were interpreted as previously. Calculation of flux rates has been discussed previously. When ouabain and ion deficient solutions were used flux calculations were based upon measurement from the initial portion only of the second phase, before the

intracellular ion content had changed significantly. All fluxes are expressed in picomoles sec^{-1} cm^{-2}.

TABLE 4(iv).

Effects of low temperature and ouabain on flux rates of E. intestinalis in seawater in light.

	20°C	-3°C	-3°C ouabain
Na influx	37.8 ± 2.2	21.4 ± 2.6	28.7 ± 3.1
Na efflux	43.9 ± 2.7	6.1 ± 0.4	6.1 ± 0.4
K influx	91.5 ± 5.6	11.0 ± 1.2	
K efflux	81.1 ± 3.0	61.0 ± 4.5	
Cl influx	68.3 ± 4.0	11.6 ± 1.3	11.6 ± 1.6
Cl efflux	54.9 ± 3.0	48.8 ± 4.2	49.4 ± 3.7

0.5mM ouabain was used. Flux rates in picomoles cm^{-2} sec^{-1}.

TABLE 4(v).

Comparison of total measured flux in the thermodynamically active direction and the calculated passive flux in the same direction for E. intestinalis.

	Total measured	Calculated passive flux in the same direction.
Na efflux in seawater at 20°C	43.9 ± 2.7	3.12
Na efflux in seawater at -3°C	6.1 ± 0.4	8.9
Na efflux in absence of K at 20°C	14.3 ± 1.2	2.7
K influx in seawater at 20°C	91.5 ± 5.6	9.5

All fluxes were measured in the light and are in units of picomoles cm^{-2} sec^{-1}.

TABLE 4(vi).

Effects of ouabain on flux rates of E. intestinalis in the light at 20°C in sea water.

	Control	Ouabain
Na influx	37.8 ± 2.2	37.5 ± 3.9
Na efflux	43.9 ± 2.7	12.3 ± 0.7
K influx	91.5 ± 5.6	59.2 ± 4.1
K efflux	81.1 ± 3.0	81.1 ± 3.7
Cl influx	68.3 ± 4.0	68.9 ± 4.4
Cl efflux	54.9 ± 3.0	55.4 ± 3.3

0.5mM ouabain was used. Flux rates in picomoles cm^{-2} sec^{-1}.

TABLE 4(vii).

Effects of ouabain and absence of K on flux rates of E. intestinalis at 20°C in the light.

	0 mMK	10 mMK	30 mMK	60 mMK
Na efflux with ouabain present	14.3 ± 1.2	12.3 ± 1.3	13.5 ± 2.2	12.3 ± 1.3
Na influx with ouabain present	37.2 ± 2.1	37.2 ± 2.1		
Na influx with no ouabain present.	37.3 ± 2.1	36.9 ± 1.7		

0.5mM ouabain was used. Flux rates in picomoles cm^{-2} sec^{-1}.

4.4. Discussion.

As has been shown in Section 3 the main active fluxes are K and Cl influx and Na efflux. The fluxes thought to include active components are markedly decreased at low temperature, consistent with their being dependent upon metabolism; those fluxes thought to be passive on electrochemical grounds are only moderately affected by low temperature. (Table4iv). Each flux against its electrochemical potential gradient must include a small diffusional or passive component as well as a larger active component. It has been argued earlier (Section 3.3) that the latter must be active transport and cannot be coupled single-ion influx-efflux exchange pumps for each ion.

It has been assumed that the passive component of both influx and efflux of each ion can be calculated from the Goldman flux equations as described in Section 2.9. This approach

assumes that the ions assort passively and independently and does, in fact, accurately predict the cell membrane potential from the passive ion fluxes along their electrochemical potential gradients (Section 3.3). The predicted passive components are shown in Table 4(v).

Na efflux and K influx are directly coupled in many organisms through a common, ATP-dependent exchange transport system. It was therefore decided to test whether the active components of these two fluxes in E. intestinalis are linked and are dependent upon metabolism.

The only fluxes which are inhibited by ouabain are indeed K influx and Na efflux which suggests that they may be directly coupled (Table 4(vi)). The K_I for ouabain inhibition is approximately 0.03mM ouabain and inhibition is complete at 0.5mM and above (Table 4(i)). The absence of effect of ouabain on other ion fluxes, or on Na efflux at low temperature indicates that ouabain has a specific effect on metabolism-dependent Na and K transport.

The residual Na efflux of 6.1 pmoles cm^{-2} sec^{-1} is the same in the presence of ouabain and at low temperature and with both together. This suggests that the residual efflux at -3°C is entirely passive. This was tested as follows: the cell membrane potentials at 20°C and +2°C were measured, +2°C being the lowest feasible temperature for potential measurement. From these the approximate cell membrane potential at -3°C was estimated and the predicted passive Na efflux at -3°C was then calculated from the two Goldman flux equations 2.3 and 2.4. The calculated passive Na efflux at -3°C was 8.9 pmoles cm^{-2} sec^{-1} which is little larger than the observed flux. This suggests that the observed flux rate at -3°C is entirely passive, and that most of the difference in Na efflux rates at 20°C and -3°C is caused by inhibition of an active transport process by lowered temperature.

The removal of K from the external

solution decreases the Na efflux, but does not significantly affect Na influx (Table 4(vii)). The Na efflux increases as the external concentration of K is increased, to a maximum value of 47.6 pmoles cm^{-2} sec^{-1} at 60 mM K (Figure 4A). This provides further evidence for a direct link between K influx and Na efflux. The removal of K causes hyperpolarisation of the cell to -52.1 ± 2.1 mV so that it could alternatively be argued that the drop in Na efflux on removal of external K from the solution might be due to an effect on the passive component of Na efflux. However, the change in passive efflux rate calculated from the Goldman flux equation, due to the change in the cell membrane potential, is far too small to account for the large change observed in Na efflux rate. Thus the active components of the transport of Na and K are likely to be coupled directly. Active coupling of the fluxes is also supported by the fact that removal of K from a solution containing

ouabain does not further decrease the Na efflux rate, as might be expected if passive flux coupling were involved. The Na efflux and K influx are inhibited by ouabain by the same amount, 32 pmoles cm^{-2} sec^{-1}, suggesting a one-to-one coupled exchange transport by a neutral, non-electrogenic cation pump. If so, ouabain should have no effect on the cell membrane potential, as found (Table 4(iii)). This is in agreement with previous conclusions obtained from the application of the Goldman equations which indicate that the membrane potential could be simply diffusional as it was predictable solely from passive fluxes of Na, K and Cl.

At 20°C in the light, two thirds of the K influx was stable to ouabain when inhibiting maximally. This residual K influx of 59.2 $\pm$ 4.1 picomoles cm^{-2} sec^{-1} is much greater than the predicted passive component of 9.5 picomoles cm^{-2} sec^{-1}. In Section 5 it is shown that three-

quarters of the putative active part of this K influx which is so far unexplained requires the presence of chloride. There is no evidence that the remainder includes a ouabain-stable Na efflux coupled with K influx. The Na efflux is the same both in the presence of ouabain at all levels of K from 0 to 60mM (Table 4(vii)) and in the absence of both K and ouabain (Table 4(vii)).

This conclusion may be invalid, however, since the K_m of the external K concentration for Na efflux is about 0.1 μmolar which could be provided by elution of K desorbed from the cell walls even after pretreatment of cells in K-free media.

The predicted passive Na efflux, calculated as above, was 3.1 picomoles cm^{-2} sec^{-1}, whereas the observed ouabain-stable efflux was 12.3 ± 0.7 picomoles cm^{-2} sec^{-1}. The P_{Na} used for this calculation was that for passive Na influx in the presence of ouabain

itself and should therefore be appropriate. If Na is indeed moving passively out of the cell independently of other ions, as is implicit in the Goldman approach, there is a small active efflux of about 9.2 picomoles cm^{-2} sec^{-1} of unknown mechanism.

5. INVESTIGATION OF LIGHT-REQUIRING ION FLUXES.

5.1. Introduction.

In this Section the effects upon the rates of influx and efflux of K, Cl and Na, of light and darkness, DCMU*, and the absence of certain ions from the medium and combinations of these treatments are recorded. This has enabled partition of various fluxes into their several components. The extent of coupling between some of these components has been determined. Light and darkness were used to determine which fluxes were linked with photosynthetic metabolism either directly or indirectly. DCMU, which at low concentrations has been found to be an inhibitor specific to photosystem 2, (Gingrass and Lemasson, 1965) allowed the photosystem linked with light-dependent ion transport to be identified. The absence of certain ions from the solution allowed the extents to which fluxes of an ion

* 3-(3,4-Dichlorophenyl)-1,1-dimethylurea

species were dependent upon the presence of a second or third ion species in the bathing solution to be determined.

5.2. Additional Methods.

5.2a. Experimental solutions.

Ouabain was used routinely at a concentration of 0.5mM at which it had been shown to inhibit maximally (Section 4). DCMU was used at a concentration of 10^{-6}M after this had been shown to inhibit maximally by the same amount at both 10^{-7}M and 10^{-6}M.* When a "No K" or "No Na" solution was employed the chloride level was kept constant at seawater concentration by the addition of choline chloride. When a "No Cl" solution was used the K and Na levels were kept constant at seawater concentration by the addition of Na and K benzene sulphonate. The composition of the experimental media are shown in Table 5(1).

* Photosynthesis is fully inhibited by 10^{-7} and 10^{-6}M D.C.M.U.

TABLE 5(i).

Artificial solutions.

Ion	Control: as for seawater	No K	No Na	No Na and No K	No Cl
Na	471	470	0	0	471
K	10.6	0	11.0	0	10.0
Mg	53.4	53.0	53.1	53.2	53.4
Ca	10.0	10.3	10.1	10.2	10.1
Cl	550	547	548	546	0
SO_4	38.0	38.1	38.2	38.0	38.1

Concentrations are expressed in mM/l.

5.3. Results.

5.3a. Cell membrane potential.

The mean cell membrane potential of at least 50 cells in each experimental solution was determined between the interior of the protoplasm and the bathing solution. The results are given in Table 5(ii). There was no evidence for a significant voltage across the tonoplast in any solution.

TABLE 5(ii).

Cell membrane potentials recorded in different experimental solutions.

Solution	Cell membrane potential (mV)
Seawater	-42 ± 1.7
Seawater + DCMU	-42 ± 1.5
No Cl + Benzene Sulphonate	-32 ± 3.1
No K, No Na + Choline Chloride	-70 ± 2.1
No K + Choline Chloride	-53 ± 1.1
No Na + Choline Chloride	-59 ± 0.8

All measurements were made at 20°C. The potentials in each solution were the same in light and darkness.

5.3b. Fluxes.

All fluxes showed typical two phase time courses and these were interpreted and discussed as previously. When ouabain, DCMU, and ion deficient solutions were used flux calculations were based upon measurements from the initial portion of the second phase, before the intracellular ion content had changed significantly. Passive permeability values of K, Na and Cl have been calculated as discussed previously, (Section 2.9).

TABLE 5(iii).

Effects of light, darkness and DCMU upon ion flux rates.

	Light	Darkness	Light + DCMU
Na influx	37.8 ± 2.2	32.3 ± 2.6	32.9 ± 2.5
Na efflux	43.9 ± 2.7	42.1 ± 3.2	41.5 ± 3.4
Cl influx	68.3 ± 4.0	24.4 ± 2.2	25.0 ± 2.1
Cl efflux	54.9 ± 3.0	53.1 ± 3.1	54.9 ± 3.3
K influx	91.5 ± 5.6	70.1 ± 5.4	69.5 ± 5.6
K efflux	81.1 ± 3.0	79.3 ± 5.4	81.1 ± 3.8

All measurements at 20°C in sea water.

Flux rates in picomoles cm^{-2} sec^{-1}.

TABLE 5(iv).

Effects of DCMU, light and darkness and absence of certain ions on Cl fluxes at 20°C.

	Control light	No K light	No Na light	No K, No Na light	No K, No Na light+DCMU	No K, No Na darkness
Cl influx	68.3±4.3	48.8±3.7	62.8±5.1	40.8±3.1	24.4±2.68	24.4±2.5
Cl efflux	56.7±4.1	54.3±3.5	51.2±3.7	42.7±5.1	38.4±4.3	40.2±5.0

Flux rates in picomoles cm^{-2} sec^{-1}.

TABLE 5(v).

Effects of No Cl, DCMU and No K on Na and K flux rates at 20°C.

	Control light	No Cl light	No Cl darkness	No K light	Control darkness	Control + DCMU.
Na influx	37.2±2.7	32.3±1.9	32.3±1.8	37.8±2.4	32.3±1.9	32.3±1.6
Na efflux	43.3±2.5	41.0±2.8	41.1±2.8	11.9±1.2	42.1±3.0	41.0±3.1
K influx	89.7±6.1	51.8±3.4	52.5±3.5	--------	70.1±5.4	70.1±5.8
K efflux	79.9±4.5	78.0±3.9	77.5±3.5	--------	79.3±5.4	79.0±5.1

Flux rates in picomoles cm^{-2} sec^{-1}.

TABLE 5(vi).

Effects of ouabain and absence of Cl on ion flux rates.

	Control	Control + ouabain	Ouabain, No Cl.
K influx	89.7 ± 6.1	59.0 ± 4.0	19.5 ± 0.9
K efflux	79.9 ± 4.6	81.1 ± 3.7	71.3 ± 5.1
Na influx	37.2 ± 2.4	37.8 ± 2.1	31.1 ± 2.5
Na efflux	43.9 ± 2.7*	12.2 ± 6.7	----------

*measured in seawater

All measurements at 20°C in light.

Flux rates in picomoles cm^{-2} sec^{-1}.

5.4. Discussion.

Darkness and DCMU did not affect the active efflux of Na, the energy for which therefore need not derive directly from any photochemical system. By contrast these treatments decreased the active influxes of K and Cl and also the passive influx of Na (Table 5(iii)). This suggested that either components of all these fluxes were directly linked with photosynthesis or that one or more was directly linked and the other fluxes were, through dependence upon these, indirectly linked. Since DCMU, an inhibitor of photosystem 2, had the same effect as darkness the link with metabolism appears to be through photosystem 2 rather than photosystem 1. ~~or carbon metabolism.~~ Active Cl influx has previously been shown to depend upon photosystem 2 in other algae as well, (MacRobbie, 1964 and 1966, Raven, 1967). A similar dependence of some of

the K influx upon photosystem 2 was found in Hydrodictyon by Raven (1968).

5.4a. The chloride influx.

Chloride influx occurs against the electrochemical gradient (Section 3.3) and would therefore include a large active as well as a small passive transport component. If for the moment the standard errors associated with each mean flux rate are ignored, the Cl influx could be subdivided in two ways as follows: first experimentally, into a light-requiring fraction of 43.9 picomoles cm^{-2} sec^{-1} sensitive to DCMU and a cation-requiring light fraction of 27.5 picomoles cm^{-2} sec^{-1} with specific components associated with Na and K (Table 5(iv)). Secondly from an electro-chemical view point, a passive influx component of 15.2 picomoles cm^{-2} sec^{-1} would be predicted from the assumptions of the Goldman flux equations; if this were to be subtracted from

the total Cl influx, the active Cl influx would be 53.7 picomoles cm^{-2} sec^{-1}.

Let us consider first whether the cation-requiring component also requires light. If these two requirements were independent then the absence of both light and cations should together decrease the Cl influx by the sum of the effects of each separately (by 27.5 for cations +43.9 for light) to a negative influx of 3.7 picomoles cm^{-2} sec^{-1}. If, however, the larger light-requiring fraction included all the smaller cation-requiring fraction, the Cl influx in the absence of both requirements should still be about 24.4 picomoles cm^{-2} sec^{-1}. The latter is the case, (Table 5(iv)). Thus the light-requiring Cl influx must be divided into two components, one requiring cations and the remainder not. The cation-requiring component is unlikely to be electrogenic, as the membrane potential is the same in light and darkness. The mean residual light-requiring Cl influx which is

independent of these cations is 15.8 picomoles cm^{-2} sec^{-1}. This flux component is also unlikely to be electrogenic, as the observed membrane potential in the absence of K and Na is the same in light and darkness.

It is simplest to assume that the large light-requiring fraction of the Cl influx occurs by active rather than passive transport for the following reasons: the majority of the Cl influx is against the electrochemical potential gradient and so must be active; and there is no significant change in the passive Cl efflux (Table 5(iii)) or in the passive driving force of the permeability for Cl between light and darkness, so that no change would be predicted in the small passive component of Cl influx.

The mean cation-requiring fraction of 27.5 picomoles cm^{-2} sec^{-1} can be subdivided into components associated specifically and almost additively with Na (5.5 picomoles cm^{-2} sec^{-1}) and K (19.5 picomoles cm^{-2} sec^{-1}),

(Table 5(iv)). While this apparent Na effect could perhaps be accounted for within the experimental variability, that for K cannot. The Cl influx in the absence of K differs significantly from that in its presence whether Na is present or not. Thus this part of the Cl influx transport system can distinguish very specifically between, and may require both, Na and K at the outside of the cell membrane.

The removal of Na from the solution, hyperpolarises the cells to -59 ± 0.8 mV. The calculated mean change of 5.5 picomoles cm^{-2} sec^{-1} in the passive Cl influx caused by this change in the membrane potential is enough to account exactly for the observed mean change in the Cl influx rate. Thus the apparent linkage between the Cl influx and the presence of external Na could be solely through the effect of Na on the membrane potential rather than on the active Cl transport. It is noteworthy that

the absence of Cl decreases the Na influx by exactly the same amount, 5.5 picomoles cm^{-2} sec^{-1}, that the absence of Na decreases Cl influx, and that both changes, if real, are almost quantitatively predictable from the changes caused in cell membrane potential.

Thus the simple assumption made above that all the light-requiring Cl influx is active may, therefore, not be valid, since at least 5.5 picomoles cm^{-2} sec^{-1} could be passive. A similar calculation made for Cl influx upon removal of K, which hyperpolarises the cells to -53 mV, indicates that some 4.8 picomoles cm^{-2} sec^{-1} may be passive and the remaining 14.7 active. Thus a total of 10.3 picomoles cm^{-2} sec^{-1} of the Na and K-requiring light sensitive Cl influx may be passive. Since the calculated passive component of Cl influx was 15.2 picomoles cm^{-2} sec^{-1} the remaining passive flux if it is real of only 4.8 picomoles cm^{-2} sec^{-1} which is unaccounted for may or may not be associated

with light-requiring Cl influx.

These predicted changes in passive Cl influx were calculated from the Goldman flux equations as discussed in Section 2.9. The Goldman-type approach assumes that the ions assort passively and independently. Since the passive movement of these different ions may not wholly be independent the equations cannot be used for quantitative predictions with any great confidence. It may, however, be unnecessary to allocate these flux components dependent upon light and cations rigidly to either active or passive transport mechanisms, since thermodynamics and mechanism are different categories. Thus while a component of the Cl influx may be thermodynamically passive it may still depend upon the cell's metabolism and may occur at separate membrane sites specific for Cl, some with Na and some with K. Whether it is assumed that the light-requiring Cl influx is wholly active, or includes passive

transport components, there remains a residual influx the nature of which cannot yet be explained. It is too large to be explained away as experimental error. If the light-requiring influx were wholly active, this residual fraction would be a mean active influx of(24.4-15.2) i.e. 9.2 picomoles cm^{-2} sec^{-1}. If the influx were partly passive the residual fraction would be an active flux of either 24.4 picomoles cm^{-2} sec^{-1} or (24.4-4.8) i.e. 19.6 picomoles cm^{-2} sec^{-1} or somewhere between these values depending upon statistical variability and upon how much of the light- dependent Cl influx is passive. It could result from a cyclic exchange turnover of Cl across the cell membrane i.e. a coupled and equivalent influx and efflux. If so, the P_{Cl} calculated from the whole efflux would be too high. There is no independent data to test this point further.

5.4b. The Potassium influx.

It has been shown that the K influx occurs against the electrochemical potential gradient and most of it must therefore be active. The mean K influx in sea water is decreased by darkness and by DCMU in the light, by the same amount, 21.4 picomoles cm^{-2} sec^{-1} (Table 5(iii)). Since neither treatment changed the membrane potential (Table 5(ii)) nor the passive efflux, no change in the small calculated passive component of 9.5 picomoles cm^{-2} sec^{-1} of K influx would be predicted. Thus part of the active K influx appears to be light-requiring. Secondly the K influx, in contrast with Na influx, is decreased much more by the absence of Cl than by darkness or by DCMU (Table 5(v)). The negligible calculated difference of 0.97 picomoles cm^{-2} sec^{-1} in the expected passive K influxes between the rates in the control and in the "No Cl" solutions is far too small to account for the observed change of 37.9 picomoles cm^{-2} sec^{-1} in the influx. Thus part of the active

K influx is dependent upon Cl in the external solution.

These two components of the active K influx could either be separate and additive, or the larger Cl-requiring fraction could include the whole smaller light-requiring part. If they were additive the mean K influx rate in darkness in the absence of Cl should be decreased by 37.9 + 21.4 to about 30.4 picomoles cm^{-2} sec^{-1}. Alternatively if the light-requiring component also required Cl, then the mean K influx in the absence of Cl should be the same in light and darkness, i.e. about 51.8 picomoles cm^{-2} sec^{-1}. The latter is found (Table 5(v)). Thus light is necessary to provide either sufficient energy or sufficient transport sites for the maximal rate of Cl dependent K influx.

The mean K influx is decreased by both ouabain, by 30.7 picomoles cm^{-2} sec^{-1}, and also by the absence of Cl from the external solution, by 37.9 picomoles cm^{-2} sec^{-1} (Table 5(vi)).

The ouabain-sensitive fraction may either be separate from the Cl-requiring fraction, or the absence of Cl may inhibit a component of the K influx which includes the whole ouabain-sensitive portion. If the fractions are additive, then ouabain in the absence of Cl should decrease the K influx to a residual 21.1 picomoles cm^{-2} sec^{-1} i.e. by (37.9 + 50) picomoles cm^{-2} sec^{-1}. If, however, the larger Cl-requiring fraction included the smaller ouabain-sensitive fraction, then the residual flux with ouabain in the absence of Cl should be 51.8 picomoles cm^{-2} sec^{-1}. The former was found.

These alternatives can also be tested by considering the Na efflux, the active portion of which appears to be linked with ouabain-sensitive K influx through a conventional K/Na coupled transport exchange system, (see Section 4.4). If the absence of Cl inhibits the ouabain-sensitive fraction of K influx, it should also decrease the fraction of active Na efflux linked

with it. This is not found (Table 5(vi)) although Na efflux is greatly inhibited by ouabain it is hardly changed by the absence of Cl. Thus the fraction of K influx coupled with this Na efflux is therefore unlikely to be Cl requiring.

Thus the active K influx contains at least two major components. One of 30.7 picomoles cm^{-2} sec^{-1} is linked with active Na efflux and sensitive to ouabain but not requiring Cl. The second is insensitive to ouabain (59 picomoles cm^{-2} sec^{-1}) and a part of it (37.9 picomoles cm^{-2} sec^{-1}) requires Cl and operates at maximal rate only in the light. If components of both the active Cl influx and active K influx are linked then from the data in Tables 5(iv) and 5(v) 2K move in with every 1Cl; the reason for this inbalance is not yet known but this system is apparently not electrogenic. This leaves an unexplained residual K influx of 21.1 $\pm$ 0.9 picomoles cm^{-2} sec^{-1} which is too

large to explain away as experimental error. Since the predicted passive fraction of the K influx should be only 9.1 picomoles cm^{-2} sec^{-1}, the remaining approximate 12.0 picomoles cm^{-2} sec^{-1} may well include a genuine and unexplained active K influx component.

5.4c. The Sodium influx.

The Na influx is thermodynamically in the passive direction along the electrochemical potential gradient. But as for active K influx, the Na influx is partly dependent upon light and upon chloride and is also inhibited by DCMU, all to the same extent of about 5.0 picomoles cm^{-2} sec^{-1}, (Table 5(v)). A similar dependence of Na influx and light has been demonstrated in Nitella by Smith (1967). This difference from the control rate is just statistically significant in all these three separate treatments, suggesting that it may be real.

A simple interpretation is that, though thermodynamically downhill, there may well be a specific membrane site for passive influx of Na coupled with active influx of Cl, activated by light and inhibited by DCMU, analagous to that for active K influx. Alternatively, the effects of light and DCMU are distinct from that of Cl since light or DCMU do not significantly change the membrane potential but the removal of Cl depolarises the cells enough to explain the observed decrease in Na influx. If this were the case, however, the effects of Cl and of either light or DCMU should be distinct and additive and when applied together the mean decrease in Na influx rate should be about (5.0 + 5.0) i.e. 10 pico-moles cm^{-2} sec^{-1}. It is not. This casts further doubt on the value of a simple Goldman type prediction of passive components of the fluxes of at least Na and Cl in Enteromorpha. The various fluxes are summarized in Figure 5A.

Figure 5A.

DIAGRAMMATIC INTERPRETATION OF ION FLUXES IN E. INTESTINALIS IN SEA WATER IN THE LIGHT AT 20°C.

Na influx

37.8 — 32.3 Passive:

37.8 — 5.5 ? Associated with Cl influx; requires light.

Na efflux

43.9 — 31.6 Active: Associated with K influx; ouabain sensitive.

43.9 — 9.2 Active: Unexplained.

43.9 — 3.1 Passive: Calculated from Goldman Equation.

K efflux

81.1 All Passive.

Cl efflux

54.9 All Passive.

Figure 5A continued.

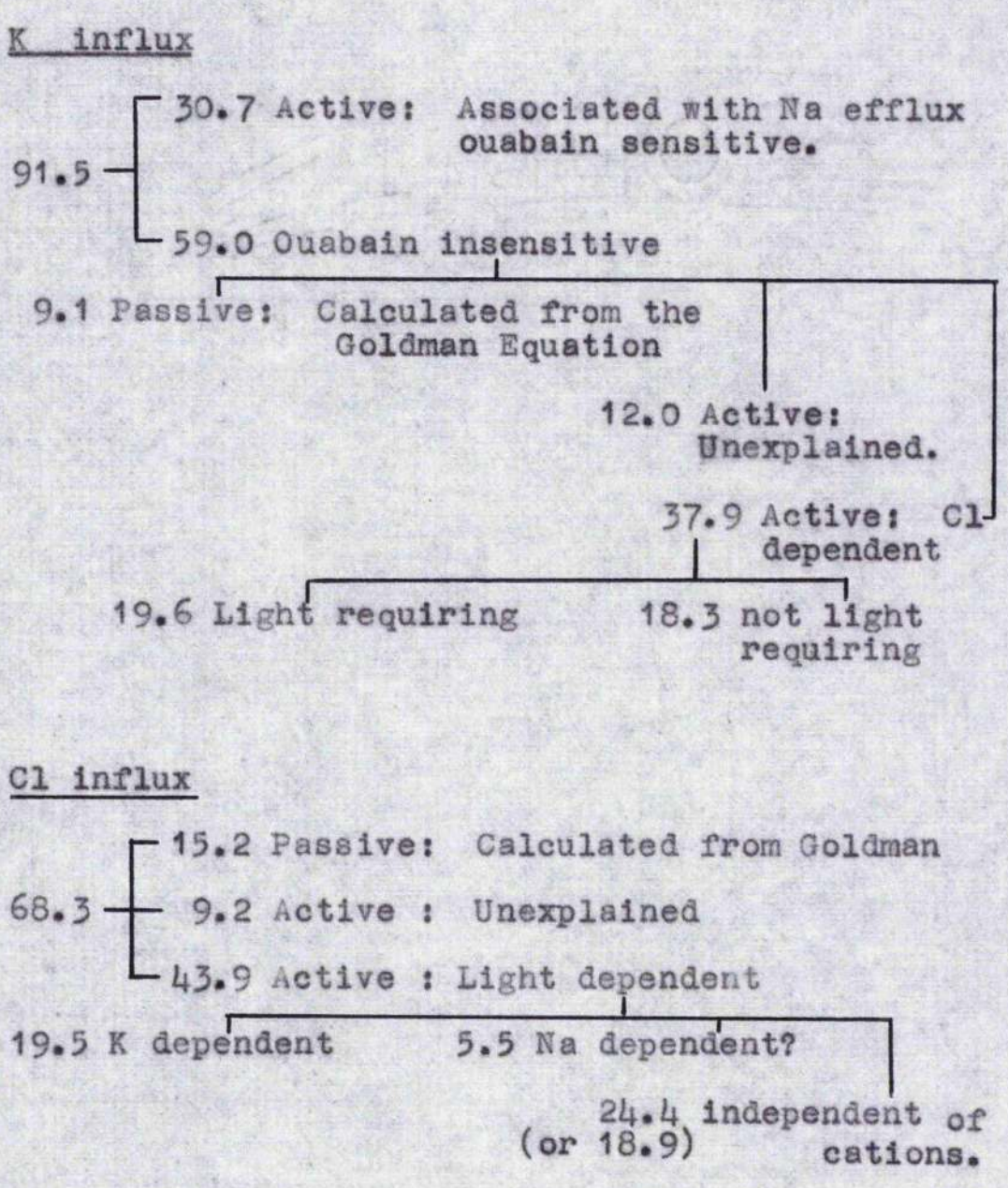

In Figure 5A the fluxes are in units of pico-moles cm^{-2} sec^{-1}.

Note small discrepancies in values may arise in cases where the flux rates measured in a "control" solution were not exactly the same as those measured in sea water under the same conditions.

6. EFFECTS OF VARYING SALINITIES ON IONIC RELATIONSHIPS.

6.1. Introduction.

E. intestinalis is found not only in sea water, but also in fresh water ponds and lochs. A single thallus can adapt to and grow in media ranging in salinity from fresh water to that of sea water. In this section the effect of varied salinity of the external medium on the ionic relationships of *E. intestinalis* is reported. Data for ion flux rates, ion concentrations and membrane potentials have been used to investigate how this species regulates its internal ionic status and to suggest what factors may allow the alga to inhabit areas of such widely varying salinity.

6.2. Additional Methods.

6.2a. Plant material and solutions.

Three types of plant material were used for these experiments. Two types of mature sporophyte plant material had been grown, in the laboratory, from the same collection of spores produced by the same parent thalli. "Equilibrated" thalli were grown in natural, filtered sea water and then transfered to various dilutions of sea water for 24 hours to equilibrate before the beginning of experiments. "Cultivated" thalli were grown throughout in various dilutions of fresh natural, filtered sea water. A third type, "field" thalli, were collected from the Kinnesburn estuary, St. Andrews, and grown in the laboratory in the dilutions of sea water in which they had been found. These dilutions were also used to grow the cultivated thalli. Experimental treatment of each type was the same and

comparison of corresponding plants from the three series has been made.

6.2b. Calculation of membrane potentials.

The Nernst equation (6.1) was used to calculate membrane potentials, the Ussing-Teorell equation (1.1) could not be used as not all the ion flux rates were known at all dilutions.

$$E_{jn} = \frac{RT}{ZF} \log_e \frac{Co}{Ci} \quad - - - \quad 6.1$$

where E_{jn} = E calculated from Nernst equation,

Co = external ion concentration,

Ci = internal ion concentration,

and other symbols have their usual meaning (see page 6).

A sample calculation is shown in Appendix 1.

6.3. Results.

6.3a. Cell membrane potential.

The mean cell membrane potential of at least 50 cells in each experimental solution was determined between the interior of the protoplasm and the bathing solution. (see Tables 6(ia), 6(ib), 6(ic)). There was no evidence for a significant voltage across the tonoplast in any solution.

6.3b. Fluxes.

Typical two-phase time courses of tracer ion fluxes were obtained for all three ions from cells in all salinities and were interpreted as previously.

TABLE 6(ia).

Internal and external Potassium concentrations, measured and calculated membrane potentials.

Plants equilibrated before use ("Equilibrated" thalli)

	Co (mM)	Ci (mM)	Measured E_m (mV)	Calculated E_{jn} (mV)	ΔE
100%	10 ± 0.8	450 ± 25.4	-42 ± 1.5	-95.7	+54
50%	5.1 ±0.5	240 ± 16.1	-45 ± 1.7	-97.4	+53
10%	0.9 ± 0.09	50.1 ± 3.6	-48 ± 2.0	-100.9	+53
5%	0.45 ± 0.03	25.2 ± 2.4	-51 ± 3.1	-98	+47
1%	0.09 ± 0.005	6.0 ± 0.39	-59 ± 3.6	-105.6	+47
0.5%	0.046 ± 0.008	3.2 ± 0.25	-65 ± 4.7	-107.0	+42
0.1%	0.001 ± 0.0001	0.83 ± 0.08	-75 ± 8.6	-110.2	+35

Where E_{jn}, E_m and E have their usual meanings, see page 42.

TABLE 6(ia) continued.

Plants grown in dilute solutions ("Cultivated" thalli).

	Co (mM)	Ci (mM)	Measured E_m (mV)	Calculated E_{jn} (mV)	ΔE
A	2.0 ± 3.6	100.3 ± 8.6	-48 ± 2.6	-97.0	+49
B	0.44 ± 0.041	26.4 ± 3.0	-52 ± 3.1	-100.9	+48
C	0.22 ± 0.032	14.1 ± 0.8	-56 ± 3.4	-102.6	+47
D	0.11 ± 0.016	7.2 ± 0.4	-58 ± 3.9	-104.4	+47
E	0.04 ± 0.007	3.0 ± 0.3	-62 ± 5.0	-108.4	+46
Plants taken from burn ("Field" thalli)					
G	2.0 ± 3.6	99.7 ± 9.3	-48 ± 3.0	-92.8	+45
H	0.44 ± 0.041	25.9 ± 2.6	-51.7 ±3.2	-103.4	+52
J	0.22 ± 0.032	14.0 ± 0.9	-56 ± 3.6	-104.4	+48
K	0.11 ± 0.016	7.0 ± 0.38	-58.2 ± 4.1	-105.0	+47
L	0.04 ± 0.007	3.1 ± 0.29	-61 ± 6.0	-108.6	+48

TABLE 6(1b).

Internal and external Sodium concentrations, measured and calculated membrane potentials.

Plants equilibrated before use ("Equilibrated" thalli).

	Co (mM)	Ci (mM)	Measured E_m (mV)	Calculated E_{jn} (mV)	ΔE
100%	460 ± 27.1	260 ± 18.1	-42 ± 1.5	+14.5	-56
50%	232 ± 15.6	131 ± 8.1	-45 ± 1.7	+14.5	-59
10%	45.0 ± 5.1	28.1 ± 2.2	-48 ± 2.0	+12.1	-60
5%	20.0 ± 1.3	13.3 ± 1.1	-51 ± 3.1	+10.5	-62
1%	4.6 ± 0.27	3.4 ± 0.29	-59 ± 3.6	+7.54	-66
0.5%	2.1 ± 0.14	1.4 ± 0.08	-65 ± 4.7	+7.0	-72
0.1%	0.41 ± 0.04	0.36 ± 0.03	-75 ± 8.6	+3.4	-78

Where E_{jn}, E_m and E have their usual meanings, see page 42.

TABLE 6(ib) continued

Plants grown in dilute solutions ("Cultivated" thalli)

	Co (mM)	Ci (mM)	Measured E_m (mV)	Calculated E_{jn} (mV)	ΔE
A	92 ± 7.4	56.1 ± 4.2	-48 ± 2.6	+11.1	-59
B	21.1 ± 1.6	13.9 ± 1.4	-52 ± 3.1	+10.4	-62
C	9.9 ± 0.84	6.5 ± 0.5	-56 ± 3.4	+9.9	-66
D	5.6 ± 0.41	4.0 ± 0.19	-58 ± 3.9	+8.12	-66
E	3.1 ± 0.26	2.4 ± 0.14	-62 ± 5.0	+6.3	-68
Plants taken from burn ("Field" thalli)					
G	92 ± 7.4	55.9 ± 4.1	-48 ± 3.0	+12.7	-61
H	21.1 ± 1.6	13.6 ± 1.3	-51.7 ± 3.2	+11.6	-63
J	9.9 ± 0.84	6.0 ± 0.51	-56 ± 3.6	+12.7	-69
K	5.6 ± 0.41	4.0 ± 0.16	-58.2 ± 4.1	+8.12	-66
L	3.1 ± 0.26	2.1 ± 0.10	-61 ± 6.0	+9.8	-71

TABLE 6(ic).

Internal and external Chloride concentrations, measured and calculated membrane potentials.

Plants equilibrated before use ("Equilibrated" thalli)

	Co (mM)	Ci (mM)	Measured E_m (mV)	Calculated E_{jn} (mV)	ΔE
100%	560 ± 30.1	370 ± 20.1	-42 ± 1.5	-11.1	-31
50%	284 ± 17.1	220 ± 18.1	-45 ± 1.7	-6.3	-38
10%	56.1 ± 3.8	42.1 ± 5.6	-48 ± 2.0	-6.9	-41
5%	27.9 ± 1.9	21.9 ± 1.4	-51 ± 3.1	-6.0	-45
1%	5.5 ± 0.29	4.6 ± 0.21	-59 ± 3.6	-4.5	-54
0.5%	2.1 ± 0.19	1.7 ± 0.06	-65 ± 4.7	-5.0	-60
0.1%	0.52 ± 0.06	0.46 ± 0.04	-75 ± 8.6	-3.1	-72

Where E_{jn}, E_m and E have their usual meanings, see page 42.

TABLE 6(ic) continued.

Plants grown in dilute solutions ("Cultivated" thalli)

	Co (mM)	Ci (mM)	Measured E_m (mV)	Calculated E_{jn} (mV)	ΔE
A	98 ± 7.1	80 ± 6.4	-48 ± 2.6	-6.0	-39
B	24.5 ± 2.0	18 ± 1.4	-52 ± 3.1	-8.0	-44
C	12.7 ± 1.0	10.9 ± 6.0	-56 ± 3.4	-4.0	-53
D	7.4 ± 0.6	6.5 ± 0.32	-58 ± 3.9	-3.3	-54
E	3.9 ± 0.31	3.6 ± 0.26	-62 ± 5.0	-2.3	-58
Plants taken from burn ("Field" thalli)					
G	98 ± 7.1	80 ± 6.5	-48 ± 3.0	-6.0	-42
H	24.5 ± 2.0	17 ± 1.6	-51.7 ± 3.2	-7.5	-44
J	12.7 ± 1.0	10.6 ± 5.8	-56 ± 3.6	-4.6	-51
K	7.4 ± 0.6	6.8 ± 0.34	-58.2 ± 4.1	-3.3	-55
L	3.9 ± 0.31	3.4 ± 0.20	-61 ± 6.0	-3.4	-57

TABLE 6(ii).

Internal ionic concentration ratios over a range of salinities.

Sample	$\frac{Cli}{Clo}$	$\frac{Nai}{Nao}$	$\frac{Ki}{Ko}$	$\frac{Nai + Ki}{Cli}$	$\frac{Ki}{Nai}$
100%	0.66	0.50	45	1.9	1.7
50%	0.73	0.58	48	1.7	1.8
10%	0.76	0.61	51	1.8	1.7
5%	0.78	0.65	55	1.7	1.9
1%	0.84	0.71	56	2.0	1.8
0.5%	0.85	0.70	70	1.8	2.3
0.1%	0.90	0.89	80	2.4	2.1
A	0.80	0.60	50	1.9	1.7
B	0.76	0.66	60	2.4	1.8
C	0.80	0.68	63	1.8	2.1
D	0.83	0.71	65	1.8	2.3
E	0.85	0.78	70	1.5	1.3
G	0.81	0.61	49.8	1.9	1.8
H	0.69	0.64	58.8	2.3	1.9
J	0.84	0.61	63.6	1.8	2.3
K	0.91	0.71	63.6	1.6	1.8
L	0.88	0.67	77.5	1.5	1.5

TABLE 6(iii).

Comparison of sum total of K, Cl and Na both internally and externally over the whole salinity range.

% Sea water	ΣCo	ΣCi
100	1030	1080
50	521	691
10	102	120
5	48.5	59
1	10.2	14.0
0.5	4.2	6.1
0.1	0.93	1.65

TABLE 6(iv).

Internal ion ratios in solutions differing from sea water in Na/K ratio.

Sample	Ko	Ki	$\frac{Ki}{Ko}$	Nao	Nai	$\frac{Nai}{Nao}$	$\frac{Ki}{Nai}$	Clo	Ci	$\frac{Cli}{Clo}$
N	10	450	45	470	260	0.55	1.7	480	400	0.83
O	30	1000	33.3	450	240	0.54	4.2	479	400	0.83
P	60	1500	25.0	415	210	0.50	7.1	480	403	0.84
R	100	2000	20.0	380	60	0.16	33.3	480	406	0.85

TABLE 6(v).

Ion flux rates over a range of salinities at 20°C in the light.

	Dilution of sea water					
Ion flux	100%	50%	10%	5%	1%	0.5%
Na influx	37.8±2.2	15.9±1.2	2.1±0.13	0.24±0.014	0.08±0.006	0.07±0.0043
Na efflux	43.9±2.7	18.3±1.3	2.7±0.18	0.26±0.015	0.11±0.006	0.09±0.0047
Cl influx	68.3±4.0	30.5±2.4	4.6±0.24	0.47±0.030	0.17±0.008	0.14±0.0086
Cl efflux	54.9±3.0	24.4±2.2	3.7±0.22	0.39±0.030	0.14±0.009	0.12±0.0091
K influx	91.5±5.6	-	5.5±0.67	-	-	0.15±0.0088
K efflux	81.1±3.0	-	4.6±0.50	-	-	0.13±0.0103

Flux rates expressed in picomoles cm^{-2} sec^{-1}.

TABLE 6(vi).

Permeability values and ratios and calculated E Goldman values over a range of salinities.

% Seawater	P_K	P_{Na}	P_{Cl}	$E_{Goldman}$	$E_{measured}$	P_{Na}/P_K
100%	503×10^{-9}	40×10^{-9}	72×10^{-9}	-42.8	-42 ± 1.5	0.081
10%	254×10^{-9}	22.0×10^{-9}	30.5×10^{-9}	-45.9	-48 ± 2.0	0.086
0.5%	205×10^{-9}	12.2×10^{-9}	27.4×10^{-9}	-58.0	-65 ± 4.7	0.070

Permeability values expressed in cm sec^{-1}.

TABLE 6(vii).

Comparison of minimal total work done in ion transport at varying salinities.

% Sea water	ΔE	$\Delta\bar{\mu}j$	Active flux	Total work ($\Delta\bar{\mu}j$xflux)	Ion
100	54	5205	91.5	476257	
10	53	5114	5.5	28127	Potassium
0.5	42	4048	0.15	607	
100	56	5404	43.9	237235	
10	60	5784	2.7	15616	Sodium
0.5	72	6940	0.09	62	
100	31	2988	68.3	204080	
10	41	3956	4.6	18197	Chloride
0.5	60	5790	0.14	810	

Flux rate is expressed in units of picomoles cm^{-2} sec^{-1}.

ΔE is expressed in mV

$\Delta\bar{u}j$ is expressed in joule $mole^{-1}$

6.4. Discussion

Occurrence of *E. intestinalis* over a remarkably wide salinity range could be due either to a phenotypic adaptability of existing thalli or to selection of genotypes each suitable only for a small salinity range.

Several lines of evidence indicate that genotype selection is not necessary and that phenotypes are extremely adaptable. Single thalli were always found to adapt in both laboratory and field to increasing and decreasing salinities over the whole range from 100 to 0.1% sea water. This adaptation was such that even the mean intracellular ion concentrations and membrane potentials of "cultured" and "equilibrated" thalli bore exactly the same quantitative relationship to varied external salinity as did those of thalli taken from the field.

Furthermore, all estuarine plants appear to be derived from spores from marine

plants, since thalli growing in the field in sites of low salinity have never been observed to release spores. Marine plants will release spores only at salinities very close to that of sea water: even 50% sea water appears to be totally inhibitory. Both gametes and zoospores transferred to low salinities immediately after release all burst, osmotically. After about 6 hours in sea water, however, the spores can settle and grow in salinities even as low as 0.1% sea water without damage. Finally the limit of distribution of the alga, in this estuary, is only as far as the upper tidal reaches where spores could be carried by incoming tides.

The values of ΔE for each ion (Tables 6(ia), 6(ib), 6(ic)) indicate that K and Cl are actively imported and Na actively exported from the cells over the whole range of salinities. It has been shown that each ion flux, against its electrochemical potential gradient, contains a large active component and not merely

a coupled exchange of each ion.

While the ratio of Ci/Co, for each ion, increases with increasing dilution, the ratios of the internal ions to one another remain reasonably constant in all 3 types of plants at all dilutions, (Table 6(ii)). The total absolute internal concentrations of ions fall with salinity but are high enough at all dilutions to give a small positive turgor, (Table 6(iii)). However, even maintenance of a small positive turgor at all salinities is not essential: thalli remain viable for more than a month when plasmolysed and kept in concentrated sea water, and will grow on return to normal salinities. The growth then produces false branching owing to disruption of intercellular connections while plasmolysed, many of the cells producing new lateral thalli: such forms are occasionally found in the field. Thus this species tolerates a very wide range of internal ion concentrations and a limited

range of Ci/Co ratios. Even a constant internal ionic composition is unnecessary as this varies widely in thalli which remain healthy in solutions of greatly varied external ionic ratio, (Table 6(iv)). This tolerance of a wide range of internal K/Na ratios appears not to depend upon a constant cytoplasmic and varying vacuolar cation composition. If, for example, with increasing dilution, the level of K in the cytoplasm remained almost constant and that of Na fell, while in the vacuole the ratio of Na to K rose, then efflux curves for Na might show a third, slower phase in highly diluted sea water. As they do not, reasons for tolerance of varying internal K/Na ratios are not yet known. Thus its ionic relationships *per se* do not appear to be critical for viability of *E. intestinalis*; in this respect it is remarkably flexible.

It is worthy of note that in a majority of marine algae generally the concentration of

Na is lower, that of Cl similar and that of K greater than in sea water, (Gutknecht and Dainty, 1968). Fresh water algae by contrast are noticeably less selective in general against Na and for K, and accumulate all three major ions; this is also true of many higher plants. Marine algae generally accumulate salts to total concentrations relatively little more than in their environment, and have fairly low positive turgor. Characean fresh water algae and higher plants generally accumulate total salts more strongly and have higher turgor pressures in their natural media. In both these respects, E. intestinalis is truly a marine alga even when growing in fresh water. 0.5% sea water is similar to the normal experimental medium used by others with Nitella translucens; the ratio of total intracellular (Na + K + Cl) to that in the medium is 119 for Nitella but 1.5 for Enteromorpha.

What then of the water relations of

thalli growing where large, frequent salinty changes occur? The alga could conceivably adapt to changes in salinity by changes in turgor pressure rather than in ionic content. This is not found; the net change in turgor upon transfer from sea to fresh water is temporary and followed by rapid net ion efflux until, when the cells have adapted, all the individual ion flux rates are lower than in sea water, but are still in the same ratios to each other, (Table 6(v)).

The flux rates recorded for E. intestinalis in 0.5% sea water are lower than those for Nitella in a solution of approximately the same composition (MacRobbie, 1964). Despite this, the much larger ratio of surface area (S.A.) to volume (V) of the smaller E. intestinalis cells would enable rapid adjustment of internal concentrations, whereas with the smaller SA/V ratio of the larger Nitella cells only slow adjustment of internal ionic concentration could

occur. This ability for rapid adjustment is illustrated in the turnover time of Na, i.e. time required for complete replacement of all internal Na ion. Approximate turnover times for one cell calculated from Na efflux rates in media of similar salinity are 23.0×10^2 seconds for E. intestinalis and 33.1×10^6 seconds for Nitella. This rapid adjustment of internal ions could be thought more important in an estuarine alga than in an alga, such as Nitella which experiences little change in salt concentration in its usual environment.

The membrane permeabilities calculated from the fluxes in the passive direction for each ion, together with $E_{Goldman}$ and P_{Na}/P_K ratio values are given in Table 6(vi). The $E_{Goldman}$ is within 10% of the observed membrane potential at all dilutions even in the most extreme case and it is therefore probable that passive diffusion of the three major ions determines the cell membrane potential not only in sea water but over the whole range of dilutions

studied.

The minimal work done in moving an ion j across the membrane against the gradient is given by:

$$\Delta \bar{\mu}j = Z_j F \Delta E_j \quad \_ \_ \_ \quad 6.2$$

where $\Delta \bar{\mu}j$ is the work done, Z is the algebraic valency, F is the Faraday and E_j is the difference between the membrane potential calculated from the Nernst equation and that observed; the cells were almost in flux equilibrium in each salinity used. The actual work of transporting each ion would be greater and probably be independent of $\Delta \bar{\mu}j$ if it were coupled to a quantised metabolic K driving reaction. ΔE_j increases on increasing dilution for Cl and Na (Table 6(vii)). The quantities of all three ions moved, whether expressed as a flux or as a fraction of the total intracellular ions also decrease. Thus, whether quantised or not, the minimal work done on the movement of ions by the cell decreases with the

salinity of the solution. If growth and osmotic work compete for supply of energy in the field, the decrease in the latter might contribute to the greater growth observed over the salinity range from 30-70% sea water, (see Section 7).

7. THE GROWTH OF E. INTESTINALIS OVER A RANGE OF SALINITIES.

7.1. Introduction.

Plants of E. intestinalis have been observed to grow to greater lengths in estuaries, where the salinity is less than that of sea water for at least part of the day, and where land drainage water spills onto the beach, than in 100% sea water. The greater lengths of plants in such places may be due to several factors. Additional nutrients may be present in the estuary and land drainage water, especially where these arise from or near farm land. Different genotypes may inhabit different parts of the salinity range, or the greater growth may be related to the decreased salinity.

In this section an attempt has been made to determine which of these factors affect the growth of these plants. The maximum lengths attained by plants grown from spores over a range of salinities in the laboratory

are therefore reported and compared with plants growing in the field.

7.2. Materials and Methods.

7.2a. Collection of spores.

It has been shown by Christie and Evans (1962) that spore release in *E. intestinalis* takes place three to five days before the highest tide of the lunar period, and that spores are not naturally released at any other time. Lernstein and Voth (1960) have reported that zooid discharge occurred in several species of *Enteromorpha* when excised sections of thallus were removed from stock culture and placed in fresh sea water, or when the pH of the sea water was changed to between pH 6.5 and pH 7.

The former findings of Lernstein and Voth could not be repeated although several attempts were made. While it was found that spore release in general was enhanced by increasing the pH this method was not used as it was uncertain how the resulting spores would be affected.

Several experiments were conducted to try and induce spore formation rather than to try and increase spore release. This would mean that spores would be available when required and availability would not depend upon lunar period. Methods included:- (1) drying the thalli for different lengths of time before placing in sea water at room temperature, (2) exposing the plants to different temperatures for different periods of time before placing in sea water and (3) exposing the plants to ethylene several days before placing in sea water. Spore formation was never successfully induced and the method of spore collection adopted is outlined below.

Thalli were collected from the East Sands, St. Andrews, during a three to five day period before the highest tide of the lunar period and taken to the laboratory in plastic bags. On return these plastic bags were placed in a refrigerator maintained at about 4°C and left there for 12 hours. On removal the thalli

were placed into white staining dishes containing filtered sea water at room temperature. In accordance with the findings of Christie and Evans (1962) the released biflagellate gametes moved toward the area of greatest illumination in the dish while the released zoospores did not appear to move at all, usually remaining on the bottom of the dish under the thalli from which they had been released. Both gametes and zoospores are seen as dark green clouds in separate areas of the dish.

The gametes were collected by pipette and removed to a glass tube. All the gametes obtained were collected and stored in this way. When sufficient gametes had been collected the tube was shaken and a small sample withdrawn and mounted in a small drop of I_2/KI solution and examined under the microscope. All spores examined in this way had two flagella showing them to indeed be gametes. Zoospores were never released in sufficient numbers to establish a complete range of cultures. However, the

zoospores that were collected were treated in the same way as gametes and grown alongside them in some of the culture solutions.

7.2b. Spore distribution.

Glass microscope slides smeared on one side with glycerine albumen were placed, smeared side uppermost, in white staining dishes. The dishes were then filled with filtered sea water at room temperature. Spores were removed from the spore suspension and pipetted onto the surface of the prepared slides until the slides appeared a uniform green colour. As the spores had all been well mixed before they had been placed in the dishes each dish was considered to contain a similar sample of spores. This enabled the response of the developing plants in each dish to be compared directly with plants in other dishes.

When all the dishes had been prepared in this way they were placed in a constant

temperature room maintained at 10°C and covered to exclude the light to allow the spores to settle for 24 hours.

7.2c. Culture conditions.

After the period of 24 hours in darkness the staining dishes were removed and immersed in white plastic bowls containing a series of dilutions of natural filtered sea water. These plastic bowls were placed on shelves in a culture cabinet which had been designed to give six light-tight compartments maximum ventilation. The whole cabinet was in a constant temperature room maintained at 10°C. Each of the six compartments contained three plastic bowls each with four staining dishes making a total of twelve slides per bowl. Each compartment also contained two 80 Watt warm white tubes and two 50 Watt tungsten bulbs. All the lights were controlled by time switches. Air was supplied to the water in each bowl

through plastic bubblers which were connected to an external compressed air supply. Plastic bubblers were used in preference to porous stone bubblers as the latter are not easily cleaned.

7.2d. Maintenance of cultures.

The water in which the plants were growing was changed twice each week and the bowls, staining dishes and bubblers cleaned, and washed free of any foreign matter. Where the plants grew densely on the slides and detritus, etc., had accumulated the plants were cleaned by squirting sea water from a wash bottle at the accumulated material while the slides were immersed in sea water. Cleaning the plants in this manner once a week was found to be satisfactory. The plants appeared deep green and turgid and remained alive for periods of at least 4 months.

7.2e. Estimation of growth of plants grown in the laboratory.

Growth of plants in various salinities could have been estimated in several ways. The weight of plants could have been used as a parameter of growth but this would have required "cultured" plants to be detached from the slides and such plants could not then have been compared with plants still attached to the slides. In view of the length of time measurements would have to be continued and the relatively small number of plants, a parameter of growth was needed that would not reduce plant number. As the thallus is essentially an unbranched hollow tube it was decided to use length as a measurement of growth. This allowed the plants to be returned to their culture bowls for subsequent growth measurement. Considering methods of statistical analysis and the time available it was decided to measure 50 plants in each bowl once each week. A series of measurements was

therefore obtained as the plants approached their maximum lengths.

A microscope fitted with an eye piece graticule was used to measure the plants until they were two to three millimeters long, then a plastic rule calibrated in 0.5mm intervals was used. To assist in measurement of the thalli they were alligned with the use of damp tissue paper. The mean length of 50 plants was determined as was the standard error of the mean, (see Appendix 1). When there was no significant change of lengths of plants over a 4 week period this mean length was taken to be the maximum length of the plants.

7.2f. Estimation of growth of plants in the field.

Several sampling stations were established along the length of the Kinnesburn estuary, St. Andrews. At each one of these stations the mean length of the plants was determined for at least 100 plants covered by

six random throws of a 20cm^2 quadrat. This was repeated once a week for a month in mid-summer. Since no significant change in the lengths of plants was apparent over this period the mean lengths were taken to be the maximum lengths of the plants at each station.

7.2g. Additional nutrients.

In one series of experiments additional nutrients (listed below) were added to each of the diluted sea water solutions. This enabled the effect of both additional nutrients and diluted sea water upon the growth of plants to be determined.

The additional nutrients were:-

0.5 $NaNO_3$ g/l

0.75 KNO_3 g/l

0.030 Na_2HPO_4 g/l

7.3. Results.

Plants derived from zoospores and those from gametes grew at the same rate, thus any errors incurred in sampling field populations were not due to the presence of different generations, (Table 7(i)).

The maximum lengths of both plants grown from spores in the laboratory and plants growing in the field are plotted against percentage sea water in Figure 7A.

Plants grown in the laboratory and transferred from 20% to 60% sea water, before their maximum length was attained, grew to approximately the same lengths as those grown from spores in 60% sea water. Plants transferred from 60% to 20% sea water were longer when transferred than the plants in 20% sea water; these thalli did not then grow further but remained healthy indefinitely.

TABLE 7(i).

Maximum lengths of plants grown from zoospores and gametes in the same solution.

% Salinity of culture solution	Maximum lengths of plants(cm) grown from	
	Gametes	Zoospores
20	2.1 ± 0.6	2.2 ± 0.5
60	7.0 ± 1.0	6.9 ± 0.9
100	3.5 ± 0.6	3.4 ± 0.7

TABLE 7(ii).

Maximum lengths of plants after transfer to solutions of different salinity.

Salinity transfer		Length of plants(cm).		
From%	To%	on transfer	max. length attained	"control"
20	60	2.1 ± 0.2	6.7 ± 1.0	7.0 ± 1.0
60	20	5.2 ± 0.7	5.2 ± 0.7	2.1 ± 0.6

"Control" gives the maximum lengths (cm) of non-transferred plants in the solution to which the sample of plants was transferred.

Figure 7A (Opposite).

Plot of length of mature plants against % sea water. The plants that grew in the field (+) are plotted against the salinity in which they were found growing at low tide. Plants grown from spores in the laboratory, with additional nutrients (•) and without (o) are plotted against % sea water of the solution in which they were grown.

For the sake of clarity standard errors of the means are not shown but are included in Appendix 4.

FIGURE 7A

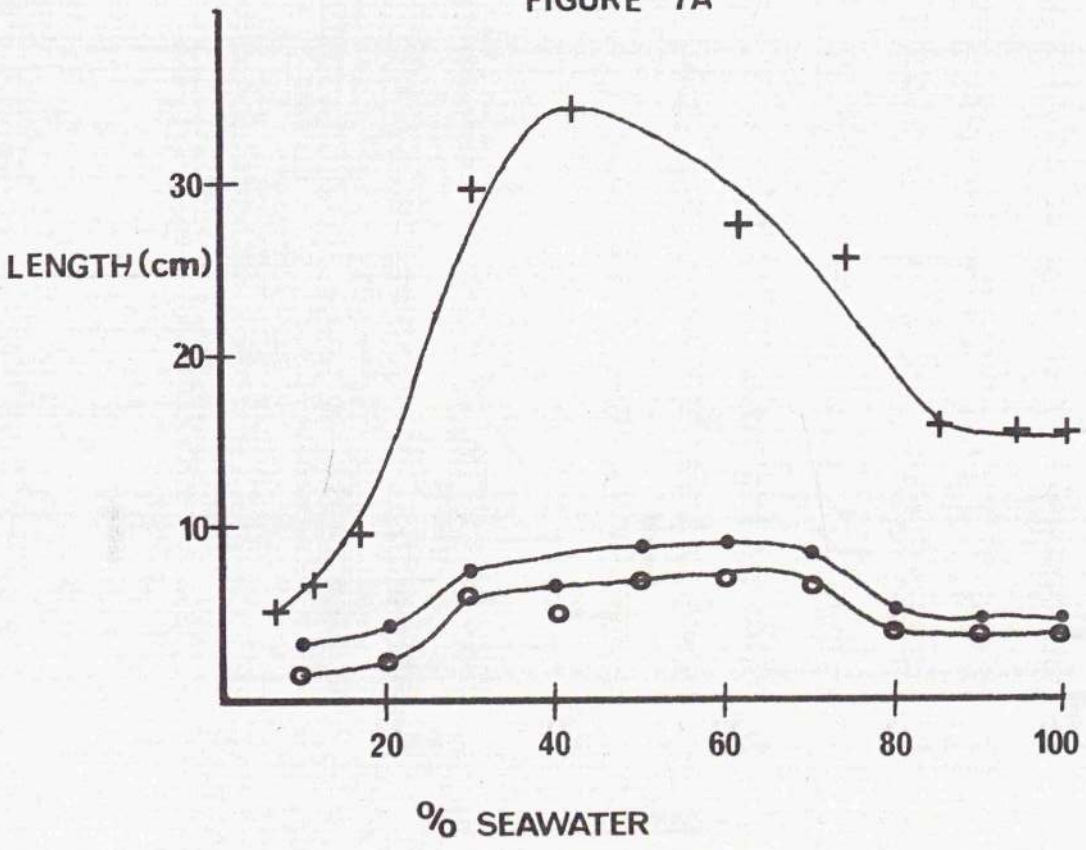

7.4. Discussion.

All estuarine plants appear to grow from spores released from marine plants growing in the sea or in positions where they experience high salinities e.g. harbour entrances. There is no evidence for different genotypes inhabiting different parts of the salinity range, this has been discussed in Section 6.4. Spores from marine plants were therefore used for growth experiments in the laboratory.

Figure 7A showed that E. intestinalis grew to greater lengths over the range 30 to 70% sea water than in 100% sea water. The greater growth in the field, than in the laboratory may be due to the higher water temperature (10°C in the laboratory and mean of about 13°C in the field) and greater light intensity (0.010 cals. min. cm^2 in the laboratory compared with minimum "cloudy day" readings of 0.61 cals. min. cm^2) and or higher nutrient content. The overall pattern of growth at varied salinities is,

however, reflected in the plants grown in the laboratory, with and without additional nutrients. This suggests that the greater growth over the range 30% to 70% sea water is related to salinity alone. The plants above and below this range would appear to be outside the range for optimum growth.

8. SUMMARY

Enteromorpha intestinalis has been found growing in a wide range of dilutions from 0.1 to 100% sea water. The ability of the plant to inhabit such an unusually wide range of salinities appears to be due to the adaptability of each individual thallus rather than to the existence of different genotypes in different parts of the salinity range. The salinity range for optimum growth appears to be between 30 and 70% sea water. The unusually wide range of salinities inhabited by this plant prompted investigation of its ionic relationships. Such a study involved measurement of ionic concentrations, cell membrane potential and ion flux rates.

The ratio of Ci/Co, for each of the major ions (K,Cl and Na), increases with increasing dilution although the total internal ionic concentration falls. However, the total internal ionic concentration is large enough,

at all salinities, to produce a small but positive turgor. A positive turgor does not appear to be essential as thalli plasmolysed in concentrated sea water will grow when returned to 100% sea water. Although E. intestinalis tolerates a wide range of ionic concentrations and a limited range of Ci/Co ratios in the field, it will remain healthy when placed in solutions with K/Na ratios different from those found in sea water. In such solutions the internal K/Na ratios differ markedly from those found in plants growing in sea water. The reason for this remarkable tolerance of varying internal K/Na ratios is not yet known.

The tracer influx and efflux curves for each ion show only two kinetic phases at all dilutions. These have been shown to be rapid ion fluxes into and out of the cell wall and slower fluxes into and out of the intracellular space. The intracellular space includes the cytoplasm and since only a single kinetic phase is found the tonoplast is thought not to be

rate limiting and all the fluxes being measured are those across the plasmalemma.

The ion flux rates are relatively high, even in low salinities, when compared with those of other algae. The small size of the cells of E. intestinalis and the small total intracellular ionic content means that turnover times for any one ion are small. Such a rapid adjustment of internal ion concentration is thought to be important in an estuarine alga, which would experience large changes in salt concentration in its natural environment.

Measurement of ion flux rates has allowed calculation of the passive permeabilities of the major ions from the Goldman flux equations for cells in different dilutions of sea water. The P_{Na} and P_K values are lower than those reported for Nitella translucens (MacRobbie 1962) but P_{Cl} is higher than that reported for most other algae. The P_{Na}/P_K value over the whole dilution range is reasonably constant and similar to that found in Chara australis

(Hope and Walker, 1961). Application of the calculated permeability values to the Goldman equation indicates that the passive diffusion of the three major ions (K, Na and Cl) may determine the cell membrane potential over the whole range of dilutions of sea water.

For each ion a flux in one direction occurs against its electrochemical potential gradient. Such a flux consists of two components one a small diffusional passive flux and the other a larger flux which has been shown to be active transport rather than a 1:1 ion exchange transport. The magnitude and sign of ΔE ($E_{observed} - E_{calculated}$) indicates that K and Cl are actively imported and Na actively exported over the whole salinity range. The site of active transport is thought to be at the plasmalemma.

The use of metabolic inhibitors, low temperature and the absence of certain ions from the bathing media and combinations of these treatments has allowed the partition of various

fluxes into their active and passive components and the interlinkages of the former to be determined.

The Na influx contains a component of about 5.5 picomoles cm^{-2} sec^{-1} which may be connected with Cl influx either directly or through the membrane potential while the rest of the flux is passive. The Na efflux has only a small passive component of about 3.0 picomoles cm^{-2} sec^{-1} while the majority of this flux is active and associated with K influx. This mechanism appears to be a typical ouabain sensitive Na/K transport mechanism found in many other algae.

The K influx and the Cl influx both contain large active and small passive components while both the effluxes appear to be entirely passive. The K influx has an active component of about 30 picomoles cm^{-2} sec^{-1} associated with the Na efflux and as discussed above is ouabain sensitive. The remainder of

the flux is ouabian insensitive and consists of a purely passive component, an unexplained active component and a second active component dependent upon the presence of Cl in the external solution. The latter is reduced to about half the original value in darkness and requires light for maximal rate. The chloride influx also contains a light dependent component part of which is dependent specifically upon Na and K and a part of which is independent of cations. 15.2 picomoles cm^{-2} sec^{-1} of the total Cl influx is purely passive and 12.0 picomoles cm^{-2} sec^{-1} unexplained active influx.

The active fluxes are interconnected in a somewhat complex manner. The fact that the fluxes remain in constant proportion to one another would suggest that this interlinking occurs over the whole salinity range. This complex interlinking together with the constant internal ionic ratios might lead to a hypothesis that constant internal ionic ratios are important for the growth of the plant. This does

not, however, appear to be the case, although necessity for strict internal sodium to potassium ratio for spore formation has not been investigated.

BIBLIOGRAPHY

Backhouse, J.K. (1967) Statistics. An Introduction to Tests of Significance. Longmans. London.

Baker, P.F., Hodgkin, A.L. and Shaw, T.I. (1962) Replacement of the axoplasm of giant nerve fibres with artificial solutions. J.Physiol.Lond. 164, 330-354.

Bernstein, L. and Nieman, R.H. (1960) Apparent free space of plant roots. Plant Physiol. 35, 589-598.

Briggs, G.E., Hope, A.B. and Robertson, R.N. (1961) Electrolytes and Plant Cells. Blackwell. Oxford.

Christie, A.O. and Evans, L.V. (1962) Periodicity in the liberation of gametes and zoospores of Enteromorpha intestinalis. Nature 193 (4811), 193-194.

Dainty, J. (1962) Ion transport and electrical potentials in plant cells. Ann.Rev.Plant Physiol. 13, 379-402.

Dainty, J. and Hope, A.B. (1959) Ionic relations in cells of Chara australis. I Ion exchange in the cell wall. Aust.J.Biol.Sci. 12, 395-411.

Dainty, J., Hope, A.B. and Denby, C. (1960) Ionic relations of cells of Chara australis. II The indiffusible anions of the cell wall. Aust.J.Biol.Sci. 13, 267-276.

Dodd, W.A., Pitman, M.G. and West, K.K. (1966) Sodium and potassium transport in the marine alga Chaetomorpha. Aust.J.Biol.Sci. 19, 341-354.

Gringrass, G. and Lemasson, C. (1965) A study of the mode of action of CMU on photosynthesis. Biochim. et Biophys.acta. 109, 67-78.

Gutkneckt, J. (1967) Ion fluxes and short-circuit current in internally perfused cells of Valonia ventricosa. J.Gen.Physiol. 50 (7), 1821-1834.

Gutkneckt, J. and Dainty, J. (1968) Ionic relations of marine algae. Oceanogr.Mar.Biol.Ann.Rev. 6, 163-200.

Hodgkin, A.L. and Katz, B. (1949) The effect of sodium ions on the electrical activity of the giant axon of the squid. J.Physiol.Lond. 108, 37-77.

Hope, A.B. (1971) Ion transport and membranes. A biophysical outline. Butterworths. London.

Hope, A.B. and Walker, N.A. (1961) Ionic relations of cells of Chara australis. IV Membrane potential differences and resistances. Aust.J.Biol.Sci. 14, 26-44.

Katchalsky, A. and Curran, P.F. (1965) Non-equilibrium thermodynamics in biophysics. Harvard University Press, Cam., Mass.

Lernstein, N. and Voth, P. (1960) Experimental control of zoid discharge and rhizoid formation in Enteromorpha. Bot.Gaz. 122, 33-44.

MacRobbie, E.A. (1962) Ionic relations of Nitella translucens.
J.Gen.Physiol. 45, 861-878.

MacRobbie, E.A. (1964) Factors affecting the fluxes of K and Cl ions in Nitella translucens.
J.Gen.Physiol. 47, 859-877.

MacRobbie, E.A. (1966) Metabolic effects on ion fluxes in Nitella translucens.
I Active influxes.
Aust.J.Biol.Sci. 19, 363-370.

Raven, J.A. (1967) Ion transport in Hydrodictyon africanum.
J.Gen.Physiol. 50 (ii), 1607-1625.

Raven, J.A. (1967) Light stimulation of active transport in Hydrodictyon africanum.
J.Gen.Physiol. 50 (ii), 1627-1640.

Raven, J.A. (1968) The linkage of light stimulated Cl influx to the K and Na fluxes in Hydrodictyon africanum.
J.Expt.Bot. 19, 233-253.

Saddler, H.W. (1970) The membrane potential of Acetabularia mediterranea. J.Gen.Physiol. 55 (6), 802-821.

Smith, F.A. (1967) Control of Na uptake into Nitella translucens. J.Expt.Bot. 18 (57), 716-723.

Sverdrup, H.U., Johnson, M.W. and Fleming, R.H. (1942) The Oceans. Prentice Hall, Inc. New York.

Teorell, T. (1949) Membrane electrophoresis in relation to bio-electrical polarization effects. Arch.Sci.Physiol. 3, 205-219.

Ussing, H.H. (1949) The distinction by means of tracers between active transport and diffusion. Acta Physiol.Scand. 19, 43-56.

West, K.R. and Pitman, M.G. (1967) Ionic relations and ultrastructure in Ulva lactuca. Aust.J.Biol.Sci. 20, 901-914.

APPENDIX 1.

This section of the appendix includes standard mathematical formulae used and sample calculations. Sample calculations have been performed for each of the major equations employed in the text. These calculations are intended to show how experimental data has been applied to the equations and therefore the calculation of every result is not reported.

App. 1.1. Determination of Standard Deviations (s)

$$s^2 = \frac{\Sigma x^2 - \frac{(\Sigma x)^2}{n}}{n - 1}$$

where x = quantity measured

n = number of observations

App. 1.2. Standard Error (S.E.)

$$S.E. = \frac{s}{\sqrt{n}}$$

App. 1.3. Standard Error of a Difference between Two Means.

$$SE^2_{(mx-my)} = \frac{s_x^2}{n_x} + \frac{s_y^2}{n_y}$$

The above formulae are taken from Backhouse(1967).

App. 1.4. Ionic Content of Cell Wall and Protoplast using Data from K Efflux.

Protoplast Content:-

specific activity of original tracer solution is 4.4×10^6 counts per milliMole K. From graph (Figure) protoplast content is $140-20=120 \times 10^4$ counts per minute (cpm) per g. tissue.

$$4.4 \times 10^6 \text{ cpm} \equiv 1 \text{ milliMole K}$$

$$1 \text{ cpm} \equiv \frac{1}{4.4 \times 10^6}$$

$$120 \times 10^4 \text{cpm/g. tissue} \equiv \frac{120 \times 10^4}{4.4 \times 10^6}$$

i.e. 27.2×10^{-2} milliMole K per g. tissue.

The total protoplast volume in 1g. tissue is $0.61 cm^3$

That is 27.2×10^{-2} milliMole Kin $0.61 cm^3$

i.e. concentration of K in protoplast is

442 milliMoles/l

Cell Wall Content:-

specific activity is the same as above.

Cell wall content (from graph, Figure)is

420-140 = 280 cpm per g. tissue.

$$\frac{280 \times 10^4}{4.4 \times 10^6} = 64.5 \times 10^{-2} \text{ milliMoles K/g. tissue}$$

Volume of cell wall per g. tissue = $0.39 cm^3$

That is 0.64 milliMoles K in a volume of $0.39 cm^3$

i.e. concentration of K in cell wall is

1653 milliMoles/l

App. 1.5. The Ussing-Teorell Equation.

$$E_j = \frac{RT}{ZF} \log_e \frac{J_{io}\, a_o}{J_{oi}\, a_i}$$

where the symbols have their usual meanings.

From data in Tables 3(iii) and 3(iv)

For Potassium

$$E_j = +58 \log \frac{81.1 \times 11}{91.5 \times 450}$$

$$E_j = +58 \log 0.021$$

$$E_j = +58 \times \bar{2}.322$$

$$E_j = +58 \times -1.68$$

$$\underline{E_j = -97.4}$$

For Sodium

$$E_j = +58 \log \frac{43.9 \times 460}{37.8 \times 260}$$

$$E_j = +58 \log 2.1$$

$$E_j = +58 \times 0.322$$

$$\underline{E_j = +18.6}$$

For Chloride

$$E_j = +58 \log \frac{54.9 \times 560}{68.3 \times 370}$$

$$E_j = +58 \log 1.2$$

$$E_j = +58 \times 0.07$$

$$\underline{E_j = +4.06}$$

App. 1.6. Flux Equations.

A sample calculation of efflux rate using chloride data for the example (see Figure 3A).

Formular used:-

$$\frac{dQ^*}{dt} = Cl_{io} \frac{Q^*}{Q}$$

where symbols have the same meaning as in the text.

dQ^*/dt is determined from the efflux graph and is expressed in counts per g. tissue/time.

Q^* is determined from the intersect of the mid point of dt and the line of the graph and is expressed as counts per g.tissue.

Q is determined from chemical analysis and is expressed as milliMoles per g. tissue.

For Cl efflux

$$Cl_{io} = \frac{dQ^*}{dt} \times \frac{Q}{Q^*} = \frac{0.09 \times 10^4}{60} \times \frac{0.222}{1.5 \times 10^4} = 2.16 \times 10^4$$

The units being:

Cl_{io} =

$$\frac{\text{counts per g.tissue}}{\text{time (seconds)}} \times \frac{\text{milliMoles per g.tissue}}{\text{counts per g.tissue}}$$

$$Cl_{io} = \frac{\text{milliMoles per g.tissue}}{\text{time (seconds)}}$$

Since one gram of tissue has a mean plasmalemma surface area of 3900cm^2

$$Cl_{io} = \frac{2.16 \times 10^{-4}}{3900}$$

$$Cl_{io} = \frac{\text{milliMoles per g.tissue per time(seconds)}}{\text{plasmalemma surface area}(cm^2) \text{ per g.}}$$

$Cl_{io} = 55.9 \times 10^{-9}$ milliMole cm^{-2} sec^{-1}

$\underline{Cl_{io} = 55.9 \text{ picomoles } cm^{-2} \text{ } sec^{-1}}$.

For Cl influx:-

Units work through in the same way as above and symbols have the same meaning as in the text.

$$\frac{dQ^*}{dt} = Cl_{oi} \frac{(Q^*max - Q^*)}{Q}$$

$$Cl_{oi} = \frac{dQ^*}{dt} \times \frac{Q}{(Q^*max - Q^*)}$$

$$Cl_{oi} = \frac{1x10^4}{60x2} \times \frac{0.222}{(29.8-22.8)x10^4}$$

$Cl_{oi} = 2.64 \times 10^{-4}$ milliMoles per g.tissue sec^{-1}

$$Cl_{oi} = \frac{2.64 \times 10^{-4}}{3900} \frac{\text{milliMoles per g.tissue } sec^{-1}}{cm^2}$$

$Cl_{oi} = 67.7 \times 10^{-9}$ milliMoles cm^{-2} sec^{-1}

$\underline{Cl_{oi} = 67.7 \text{ picomoles } cm^{-2} sec^{-1}}$.

App. 1.7. Calculation of Permeability Constants.

The sample calculation is of P_K from the Goldman flux equation. P_K is calculated from the passive flux, which in the case of K is the flux from inside to outside (efflux).

$$K_{io} = + P_K \frac{ZFE}{RT} \frac{C_i \exp(ZFE/RT)}{1-\exp(ZFE/RT)}$$

where the symbols have the same meaning as in the text.

$$K_{io} = + P_K \frac{1x96.4x-42.0}{8.31x293} \times \frac{0.450x10^9x0.1773}{1-0.1773}$$

$81.1 = + P_K \times -0.161x10^9$

$$P_K = \frac{81.1}{-0.161 \times 10^9} = 503 \times 10^{-9}$$

$P_K = 503 \times 10^{-9}$ cm sec^{-1}

App. 1.8. Calculation of E Goldman in sea water.

Data from Tables 3(iii) and 3(iv).

$$E_G = \frac{RT}{F} \ln \frac{P_{Na}(Na_o) + P_K(K_o) + P_{Cl}(Cl_i)}{P_{Na}(Na_i) + P_K(K_i) + P_{Cl}(Cl_o)}$$

where the symbols have the same meaning as in the text.

$$E_G = 25.27 \ln \frac{(40 \times 460) + (503 \times 11) + (72 \times 370)}{(40 \times 260) + (503 \times 450) + (72 \times 560)}$$

$$E_G = 25.27 \ln \frac{18400 + 5533 + 26640}{10400 + 226350 + 40320}$$

$$E_G = 25.27 \ln \frac{50573}{277070}$$

$$E_G = 25.27 \ln 0.18$$

$$E_G = 25.27 \times -1.7$$

$$E_G = -42.8$$

The membrane potential calculated from the Goldman Equation is -42.8mV.

App. 1.9. The Nernst Equation.

Sample calculation for K from data in Table 6(ia).

$$E = \frac{RT}{ZF} \log_e \frac{C_o}{C_i}$$

$E = +58 \times \log C_o - \log C_i$

$E = +58 \times \log 10 - \log 450$

$E = +58 \times 1.00 - 2.653$

$E = +58 \times -1.65$

$\underline{E = -95.7mV}$

APPENDIX 2.

App. 2. DETERMINATION OF BLOTTING PROCEDURE.

App. 2.1. Introduction.

When transferring plants from experimental solutions to Nitric acid for analysis or to planchets for counting, it is important to know how much solution is carried over on the surface of the tissue. If the amount is large it will constitute a source of error. While it is possible to dry the tissue completely by sustained heavy blotting this may well lead to loss of ions from the cell wall. It was therefore decided to remove as much solution as possible from the surface of the thallus and estimate the amount carried over. A modification of the methods employed by Bernstein and Nieman (1960) was used to determine the surface water carried over on the thallus.

App. 2.2. Materials and Methods.

A one-tenth dilution of Reeves Indian Ink was made using distilled water, sea water could not be used as this caused flocculation of the colloidal carbon. Clean pieces of thalli were placed into the sol and left for 30 seconds. This allowed the Indian Ink to replace surface water but the colloidal particles were too large to penetrate the free space. This was observed by microscopic examination of the tissue. Thus any Indian Ink subsequently eluted from the thallus had therefore come only from the surface of the tissue.

A separate thallus was split open along its entire length and then cut into lengths of about one cm. to enable both sides of the thallus to be uniformly blotted. The small pieces of known weight were then placed into the Indian Ink for thirty seconds, after which the tissue was removed, placed between

two paper tissues and the standard weight (52g) rolled over it. The pieces of tissue were then transferred for elution to 20ccs of distilled water for thirty seconds, removed, and placed in a further 20ccs for sixty seconds. The optical densities of the equilibrating sol of Indian Ink and the eluting waters were then determined using an SP 500 Unicam spectrophotometer.

Knowing the optical densities of the solutions and the dilution factors it is possible to calculate the amount of bathing solution carried over on a unit fresh weight of thallus, using the expression:-

$$H = \frac{A \times B}{(C \times D) - A}$$

where A = Optical density of eluting water

B = Volume of eluting water

C = Optical density of equilibrating sol

D = dilution factor used in determining C

H = Volume of sol carried over on the tissue

App. 2.3. Results.

The value of H was determined for 10 separate pieces of thallus. All the tissue weights and values of optical densities were corrected to 0.1g. tissue. The mean value of H was found to be 0.002 ± 0.00016 ml per 0.1g. fresh weight of tissue. Thus a mean of 0.002ml of equilibrating solution was carried over on every 0.1g. tissue.

App. 2.4. Discussion.

Since the density of the equilibrating solution is approximately unity the amount of solution carried over on the surface is 0.002g. which is less than 2% by weight. Since this method provides good duplication of results and an efficient method of blotting this procedure was established as standard for each experiment.

APPENDIX 3.

App. 3. DETERMINATION OF CELL WALL WATER FREE SPACE.

App. 3.1. Introduction.

There are several methods available for determining the apparent free space (AFS) of a tissue, these are discussed in Briggs, Hope and Robertson (1961). Several of these are based on the principle of allowing a non-electrolyte, e.g. mannitol, to exchange with the water in the AFS of the tissue and then estimating the volume of non-electrolyte in the tissue. Since the non-electrolyte is thought not to penetrate (or to penetrate very slowly) the cell membrane the volume occupied by the solution represents the AFS of the tissue. Several attempts were made to determine the volume of mannitol by weighing but this did not prove successful. Instead the AFS was determined by the radio-active tracer technique, using ^{14}C mannitol, outlined below.

App. 3.2. Materials and Methods.

The rate and amounts of influx of ^{14}C mannitol were determined using small pieces of uniform thallus (see Section 2.1) which were immersed for a known length of time in sea water containing tracer amounts of ^{14}C mannitol only, or in a solution of mannitol (approximately 0.6M) iso-osmotic with sea water, also containing ^{14}C mannitol. The rate of efflux was also determined using small pieces of uniform thallus which were equilibrated in the appropriate tracer mannitol solution, removed, then washed in the identical tracer-free solution for a known length of time. On removal from the solutions the tissue was blotted and counted as described in Sections 2.2 and 2.10.

App. 3.3. Results.

Figure App. 3A shows a plot of counts per gram of tissue against time for both sea water and the iso-osmotic mannitol solutions. In both cases a plateau is reached within one minute and is maintained at a constant value for at least one hour. The semi logarithmic plot, Figure App. 3B, showing rate of loss of tracer with time is a straight line until the counts reach a background level; a second phase is not apparent. The rate constant for elution is within the range found for elution of ions from isolated cell wall material and from the first fast phase with whole tissue. Thus mannitol is restricted to cell walls alone.

App. 3.4. Calculation of Results.

App. 3.4a. Sea water containing tracer ^{14}C mannitol:

0.1ml of this solution gives a mean value of 72820 ± 8014 cpm.

The mean number of counts in 1g. tissue was 284×10^3 cpm. (obtained from graph Figure 7A)

The mean volume of the free space occupied by the solution is therefore:-

$$\frac{0.1 \times 284\ 10^3}{72820} = 0.396 \text{ ml/g}$$

The mean volume of the free space is therefore 0.396 ml/g.

App. 3.4b. Mannitol solution iso-osmotic with sea water containing tracer ^{14}C mannitol:

0.1ml of this solution gives a mean value of 746127 ± 5142.cpm.

The mean number of counts in 1g. tissue was 296.9×10^3cpm (obtained from graph Figure 7A)

The mean volume of the free space occupied by the solution is therefore:-

$$\frac{0.1 \times 296.9 \times 10^3}{746127} = 0.392 \text{ ml/g.}$$

The mean volume of the free space is therefore

0.392 ml/g.

Figure App. 3A (Opposite).

Uptake by E. intestinalis of tracer ^{14}C mannitol in sea water (o) and ^{14}C mannitol from approximately 0.6M mannitol solution (•) plotted against time, in the light at 20°C. Each point is the mean of 6 samples and the standard error of the mean is shown by a vertical line.

FIGURE App. 3A

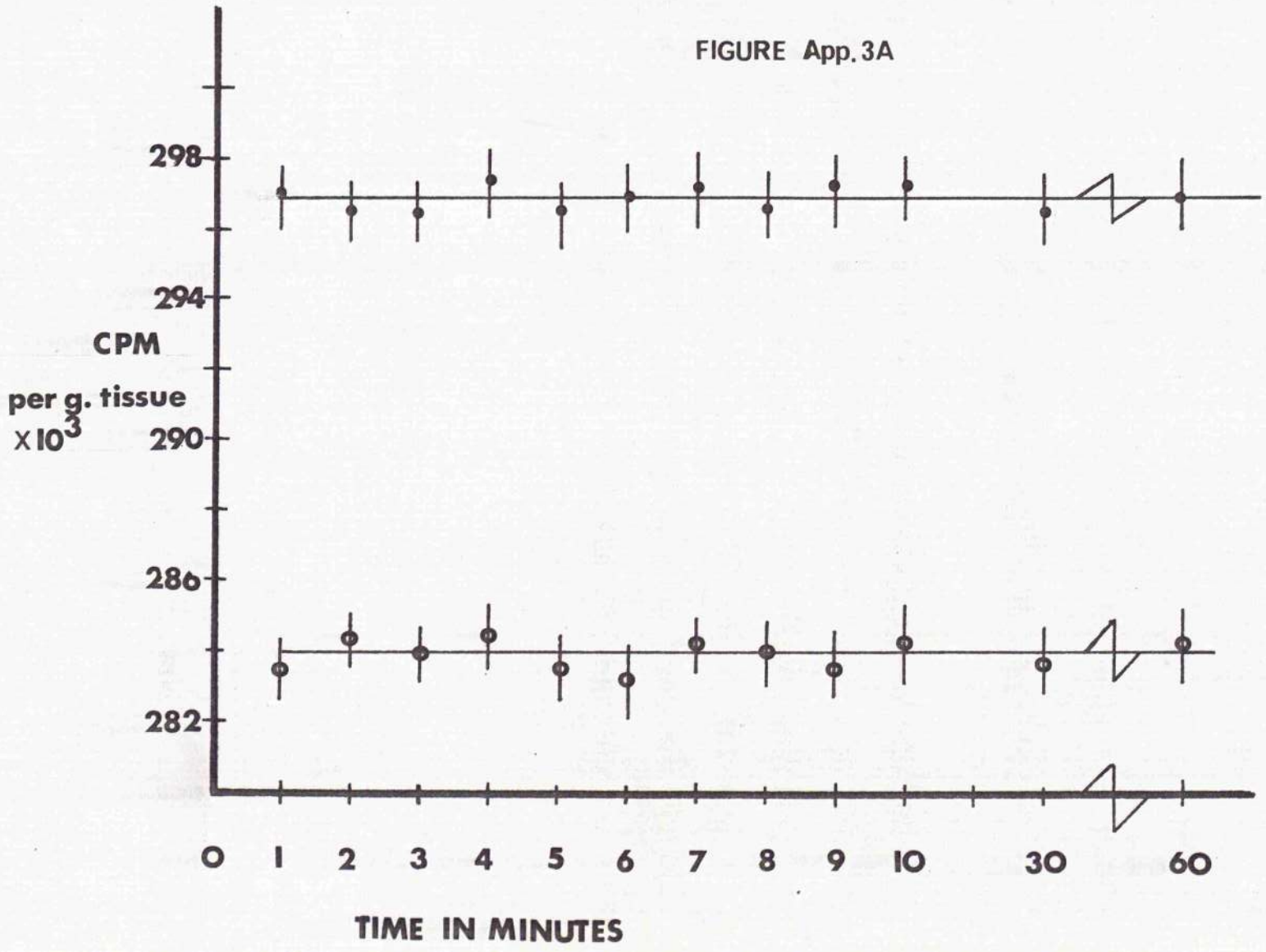

Figure App. 3B (Opposite).

Efflux of tracer ^{14}C mannitol from *E. intestinalis* cells into non-radioactive mannitol solution in the light at 20°C. Each point is the mean of 6 samples with the standard error of the mean shown by a vertical line.

FIGURE App. 3B

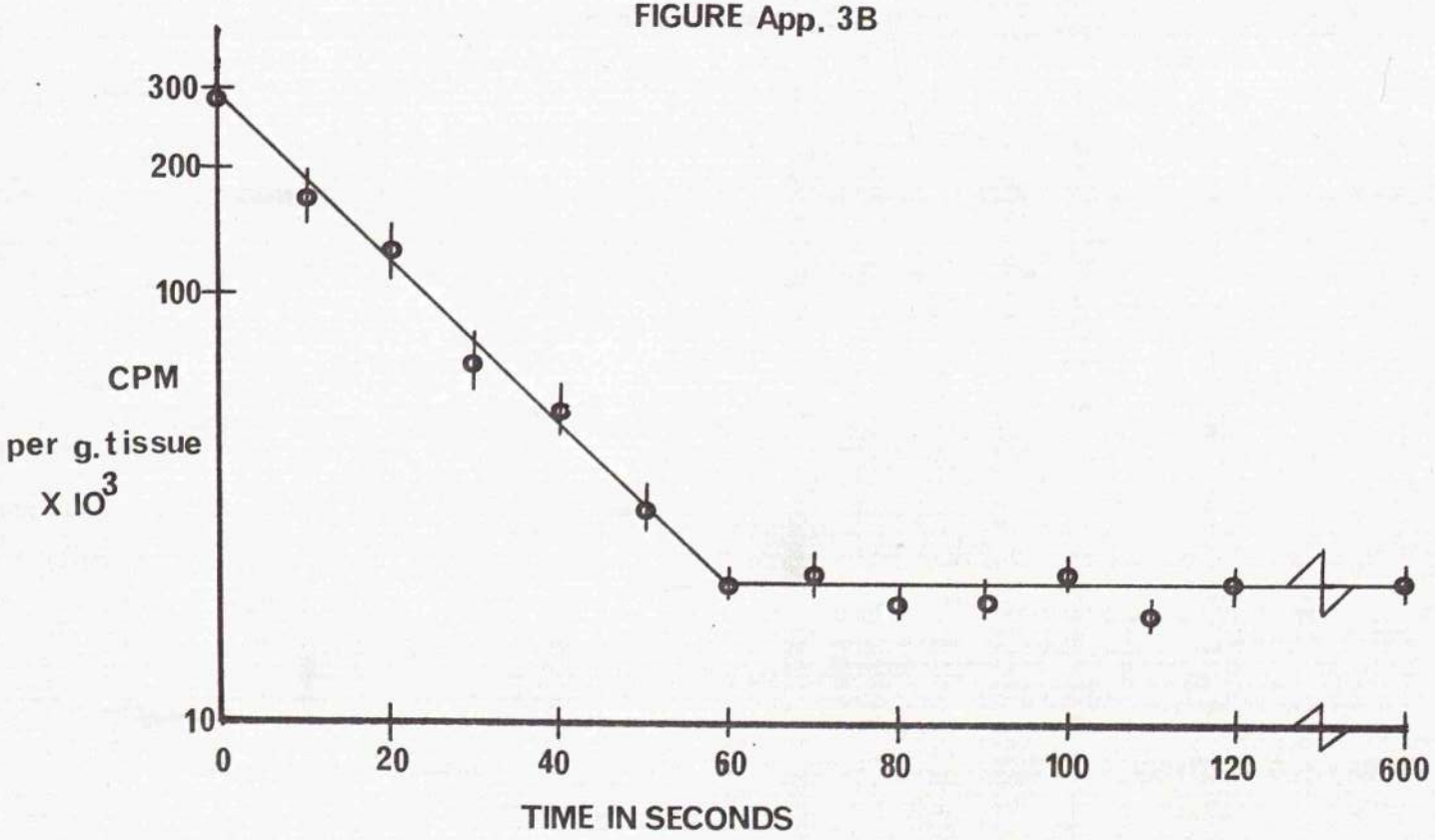

App. 3.5. Discussion.

The single phase of the efflux graph suggests that the mannitol is washed out of a single kinetic compartment. There is no second phase as would be expected if the mannitol were moved across a rate limiting membrane, such as the plasmalemma. This result suggests that the mannitol is being washed out of a single compartment which is considered to be the water free space of the cell wall. The rapid rate of isotope equilibration also supports this view. The constant value of the plateau shown on the influx graphs indicates that there is no gradual accumulation of mannitol after the initial short uptake period. This observation supports the view that tha mannitol is occupying the water free space of the cell wall and does not, at least over a one hour period, accumulate inside the plasmalemma.

The calculations of the cell wall

water free space from both sea water and mannitol values are closely in agreement with each other and with those obtained from light microscope observations.

A knowledge of the volume of the cell wall water free space allows concentrations of the ions in the cell wall to be estimated and also, with light microscope data the protoplast volume to be determined.

APPENDIX 4.

App. 4. THE STANDARD ERRORS OF THE MEAN OF POINTS PLOTTED IN FIGURE 7A.

TABLE App. 4(i).

Length of Plants (cm).

% Seawater	No additional nutrient	With additional nutrient
10	1.5 ± 0.15	3.0 ± 0.29
20	2.1 ± 0.20	4.2 ± 0.40
30	6.0 ± 0.59	7.5 ± 0.80
40	5.1 ± 0.56	6.6 ± 0.62
50	6.4 ± 0.70	9.1 ± 0.90
60	6.9 ± 0.71	9.1 ± 0.87
70	6.7 ± 0.64	8.5 ± 0.81
80	3.5 ± 0.32	3.6 ± 0.32
90	3.4 ± 0.40	4.7 ± 0.41
100	3.4 ± 0.32	4.3 ± 0.43

TABLE App. 4(ii).

% Seawater	Length of Plants in the Field(cm)
6	5.0 ± 1.0
11	6.5 ± 1.20
16	9.5 ± 0.95
30	30.0 ± 0.63
42	34.5 ± 0.67
62	27.5 ± 0.51
74	26.1 ± 0.59
85	15.5 ± 0.41
94	15.5 ± 0.40
100	15.5 ± 0.39